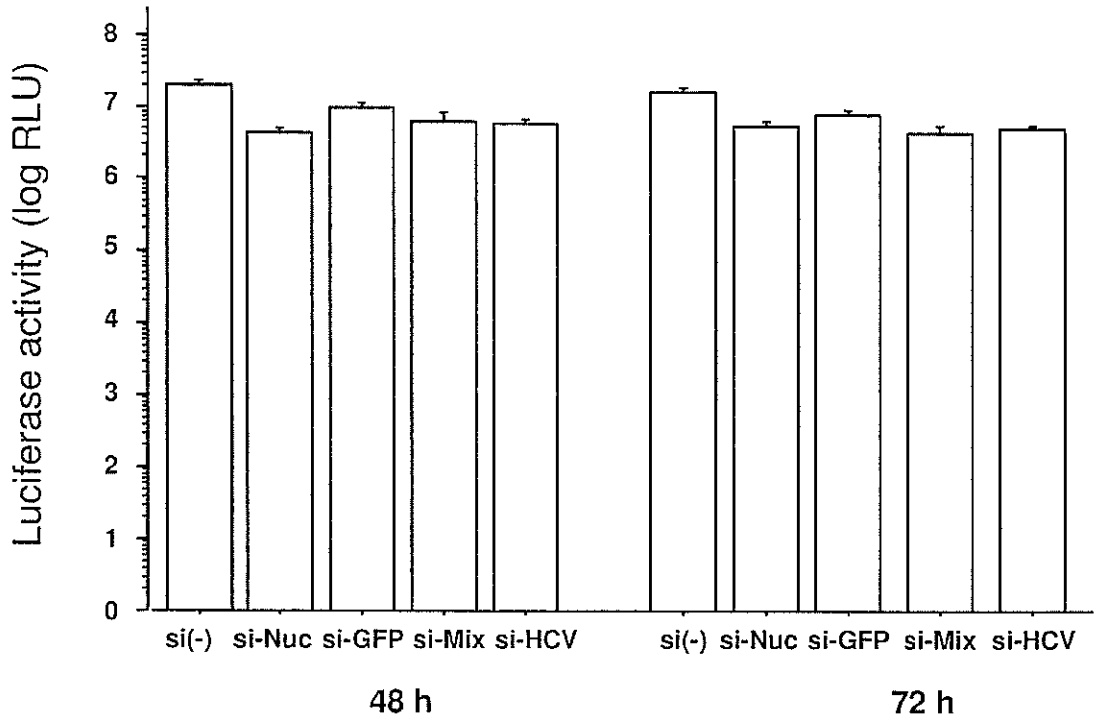

FIG. 6. Effect of suppression of endogenous nucleolin on cell proliferation. The plasmid pGL3 control, encoding the luciferase gene under the control of the CMV promoter/enhancer, was cotransfected with 2 μM of si-Mix, si-GFP, si-Nuc, si-HCV, or no siRNA [si(−)] using DMRIE-C reagent, and luciferase activity was measured 48 and 72 h after transfection. The error bars indicate the standard deviations of the results from at least three independent experiments.

We found that recombinant C-terminal nucleolin proteins can bind NS5B and inhibit its RdRp activity in a dose-dependent manner (20), suggesting that nucleolin may affect HCV replication by interacting with NS5B. The direct interaction of nucleolin with HCV NS5B in vivo and in vitro was shown to require two critical stretches of NS5B. Here, we showed that within one of these regions, aa 208 to 214, the W208 residue was critical for both binding of nucleolin and HCV replication. Transient down-regulation of endogenous nucleolin by siRNA considerably inhibited HCV replication in Huh7 cells. These results strongly indicate that nucleolin has an important role in HCV replication through its direct interaction with NS5B.

Our finding of an important positive role for nucleolin in HCV replication is apparently inconsistent with previous findings of an inhibitory role for nucleolin. It was previously reported that purified C-terminal nucleolin proteins inhibited the RdRp activity of NS5B in vitro. The latter result, however, may have been due to the use of recombinant truncated nucleolin proteins, because recombinant full-length nucleolin was not available (70). Taken together, however, these results indicate that N-terminal nucleolin may be important for the positive function of nucleolin in HCV replication, although the NS5B-binding region is within the RGG domain and RNA-binding domain 4 is at the C terminus.

Transfection of the mutant replicon containing NS5B W208A, which could not bind nucleolin, led to almost no HCV replication. By contrast, the suppression of nucleolin by siRNA moderately inhibited HCV replication, a result also observed with the transient assay using luciferase reporter replicon and G418-resistant colony formation. While HCV replication was completely inhibited by MA/W208A, replication was only partially inhibited by si-Nuc, indicating that si-Nuc can transiently suppress, but cannot eliminate, expression of endogenous nucleolin. Recently, nucleolin was reported to inhibit cell cycle progression after heat shock and genotoxic stress by increasing complex formation with human replication protein A (26). When pGL3 control or pCI-Neo was cotransfected with si-Nuc, the luciferase activity or the number of G418-resistant colonies was not reduced, strongly suggesting that the moderate inhibition of nucleolin expression did not have severe cytotoxic effects on siRNA-transfected cells. More efficient suppression of nucleolin may result in more severe inhibition of HCV RNA replication. It is therefore important to determine whether nucleolin is dispensable in mammalian cells as it is in *Saccharomyces pombe* (17) and *Saccharomyces cerevisiae* (31), since nucleolin may constitute a putative therapeutic target to inhibit HCV replication.

Using a clustered alanine substitution mutant library (CM) of NS5B, we previously showed that two stretches of NS5B amino acids, aa 208 to 214 and 500 to 506, were critical for nucleolin binding. According to the crystal models of NS5B, the former stretch is in the palm and the latter stretch is in the bottom of the thumb domain. We focused on identifying residues in aa 208 to 214 that are essential for nucleolin binding and HCV replication, as the CM mutant of aa 500 to 506 was defective in RdRp activity in vitro and HCV replication in vivo (36, 48, 49). We found that the W208 residue was critical for

both nucleolin binding and HCV replication. This residue is exposed to solvent at the edge of the palm and is not close to the catalytic pocket.

Nucleolin may stabilize monomeric NS5B, making it ready for oligomerization to NS5B, or it may facilitate the formation of a complex between NS5B and template RNA. In both cases, a substoichiometric amount of nucleolin may be required transiently at a step prior to the catalytic RdRp reaction of NS5B. Efforts to determine the contribution of amino acid residues 500 to 508 to nucleolin binding and HCV replication in vivo are ongoing and may reveal further correlations. We found that another mutant replicon, MA/K211A, reduced the number of G418-resistant colonies compared with the wild type and the other mutants. Because K211A of NS5Bt is close to the pocket of catalytic activity and did not affect binding to nucleolin, K211 may contribute to the structural integrity of the pocket or the heat-stable property of RdRp as reported previously (36).

Efficient HCV replication and infection in tissue-cultured cells by using full-length HCV RNA replicons have been reported previously (32, 63, 72). HCV replication occurs in differentiated subcellular fractions and involves dynamic complexes of structural proteins, nonstructural proteins, and HCV RNA demarcated by membrane structures. It is therefore of great interest to determine whether nucleolin is involved in such HCV-replicating intermediates in compartmented subcellular structures.

REFERENCES

1. **Alter, H. J., R. H. Purcell, J. W. Shih, J. C. Melpolder, M. Houghton, Q. L. Choo, and G. Kuo.** 1989. Detection of antibody to hepatitis C virus in prospectively followed transfusion recipients with acute and chronic non-A, non-B hepatitis. N. Engl. J. Med. 321:1494–1500.
2. **Behrens, S. E., L. Tomei, and R. De Francesco.** 1996. Identification and properties of the RNA-dependent RNA polymerase of hepatitis C virus. EMBO J. 15:12–22.
3. **Bordo, D., and P. Argos.** 1991. Suggestions for "safe" residue substitutions in site-directed mutagenesis. J. Mol. Biol. 217:721–729.
4. **Bose, S., M. Basu, and A. K. Banerjee.** 2004. Role of nucleolin in human parainfluenza virus type 3 infection of human lung epithelial cells. J. Virol. 78:8146–8158.
5. **Brunner, J. E., J. H. Nguyen, H. H. Roehl, T. V. Ho, K. M. Swiderek, and B. L. Semler.** 2005. Functional interaction of heterogeneous nuclear ribonucleoprotein C with poliovirus RNA synthesis initiation complexes. J. Virol. 79:3254–3266.
6. **Callebaut, C., S. Nisole, J. P. Briand, B. Krust, and A. G. Hovanessian.** 2001. Inhibition of HIV infection by the cytokine midkine. Virology 281:248–264.
7. **Choo, Q. L., G. Kuo, A. J. Weiner, L. R. Overby, D. W. Bradley, and M. Houghton.** 1989. Isolation of a cDNA clone derived from a blood-borne non-A, non-B viral hepatitis genome. Science 244:359–362.
8. **de Verdugo, U. R., H. C. Selinka, M. Huber, B. Kramer, J. Kellermann, P. H. Hofschneider, and R. Kandolf.** 1995. Characterization of a 100-kilodalton binding protein for the six serotypes of coxsackie B viruses. J. Virol. 69:6751–6757.
9. **Dimitrova, M., I. Imbert, M. P. Kieny, and C. Schuster.** 2003. Protein-protein interactions between hepatitis C virus nonstructural proteins. J. Virol. 77:5401–5414.
10. **Dumler, I., V. Stepanova, U. Jerke, O. A. Mayboroda, F. Vogel, P. Bouvet, V. Tkachuk, H. Haller, and D. C. Gulba.** 1999. Urokinase-induced mitogenesis is mediated by casein kinase 2 and nucleolin. Curr. Biol. 9:1468–1476.
11. **Egger, D., B. Wolk, R. Gosert, L. Bianchi, H. E. Blum, D. Moradpour, and K. Bienz.** 2002. Expression of hepatitis C virus proteins induces distinct membrane alterations including a candidate viral replication complex. J. Virol. 76:5974–5984.
12. **Ferrari, E., J. Wright-Minogue, J. W. Fang, B. M. Baroudy, J. Y. Lau, and Z. Hong.** 1999. Characterization of soluble hepatitis C virus RNA-dependent RNA polymerase expressed in *Escherichia coli*. J. Virol. 73:1649–1654.
13. **Friebe, P., and R. Bartenschlager.** 2002. Genetic analysis of sequences in the 3′ nontranslated region of hepatitis C virus that are important for RNA replication. J. Virol. 76:5326–5338.
14. **Ginisty, H., H. Sicard, B. Roger, and P. Bouvet.** 1999. Structure and functions of nucleolin. J. Cell Sci. 112:761–772.
15. **Goh, P. Y., Y. J. Tan, S. P. Lim, Y. H. Tan, S. G. Lim, F. Fuller-Pace, and W. Hong.** 2004. Cellular RNA helicase p68 relocalization and interaction with the hepatitis C virus (HCV) NS5B protein and the potential role of p68 in HCV RNA replication. J. Virol. 78:5288–5298.
16. **Gosert, R., D. Egger, V. Lohmann, R. Bartenschlager, H. E. Blum, K. Bienz, and D. Moradpour.** 2003. Identification of the hepatitis C virus RNA replication complex in Huh-7 cells harboring subgenomic replicons. J. Virol. 77:5487–5492.
17. **Gulli, M. P., J. P. Girard, D. Zabetakis, B. Lapeyre, T. Melese, and M. Caizergues-Ferrer.** 1995. gar2 is a nucleolar protein from Schizosaccharomyces pombe required for 18S rRNA and 40S ribosomal subunit accumulation. Nucleic Acids Res. 23:1912–1918.
18. **Harms, G., R. Kraft, G. Grelle, B. Volz, J. Dernedde, and R. Tauber.** 2001. Identification of nucleolin as a new L-selectin ligand. Biochem. J. 360:531–538.
19. **Hijikata, M., N. Kato, Y. Ootsuyama, M. Nakagawa, S. Ohkoshi, and K. Shimotohno.** 1991. Hypervariable regions in the putative glycoprotein of hepatitis C virus. Biochem. Biophys. Res. Commun. 175:220–228.
20. **Hirano, M., S. Kaneko, T. Yamashita, H. Luo, W. Qin, Y. Shirota, T. Nomura, K. Kobayashi, and S. Murakami.** 2003. Direct interaction between nucleolin and hepatitis C virus NS5B. J. Biol. Chem. 278:5109–5115.
21. **Hovanessian, A. G., F. Puvion-Dutilleul, S. Nisole, J. Svab, E. Perret, J. S. Deng, and B. Krust.** 2000. The cell-surface-expressed nucleolin is associated with the actin cytoskeleton. Exp. Cell Res. 261:312–328.
22. **Ikeda, M., M. Yi, K. Li, and S. M. Lemon.** 2002. Selectable subgenomic and genome-length dicistronic RNAs derived from an infectious molecular clone of the HCV-N strain of hepatitis C virus replicate efficiently in cultured Huh7 cells. J. Virol. 76:2997–3006.
23. **Kato, N., Y. Ootsuyama, H. Sekiya, S. Ohkoshi, T. Nakazawa, M. Hijikata, and K. Shimotohno.** 1994. Genetic drift in hypervariable region 1 of the viral genome in persistent hepatitis C virus infection. J. Virol. 68:4776–4784.
24. **Kato, T., T. Date, M. Miyamoto, Z. Zhao, M. Mizokami, and T. Wakita.** 2005. Nonhepatic cell lines HeLa and 293 support efficient replication of the hepatitis C virus genotype 2a subgenomic replicon. J. Virol. 79:592–596.
25. **Kibbey, M. C., B. Johnson, R. Petryshyn, M. Jucker, and H. K. Kleinman.** 1995. A 110-kD nuclear shuttling protein, nucleolin, binds to the neurite-promoting IKVAV site of laminin-1. J. Neurosci. Res. 42:314–322.
26. **Kim, K., D. D. Dimitrova, K. M. Carta, A. Saxena, M. Daras, and J. A. Borowiec.** 2005. Novel checkpoint response to genotoxic stress mediated by nucleolin-replication protein A complex formation. Mol. Cell. Biol. 25:2463–2474.
27. **Kim, S. J., J. H. Kim, Y. G. Kim, H. S. Lim, and J. W. Oh.** 2004. Protein kinase C-related kinase 2 regulates hepatitis C virus RNA polymerase function by phosphorylation. J. Biol. Chem. 279:50031–50041.
28. **Kishine, H., K. Sugiyama, M. Hijikata, N. Kato, H. Takahashi, T. Noshi, Y. Nio, M. Hosaka, Y. Miyanari, and K. Shimotohno.** 2002. Subgenomic replicon derived from a cell line infected with the hepatitis C virus. Biochem. Biophys. Res. Commun. 293:993–999.
29. **Kolykhalov, A. A., K. Mihalik, S. M. Feinstone, and C. M. Rice.** 2000. Hepatitis C virus-encoded enzymatic activities and conserved RNA elements in the 3′ nontranslated region are essential for virus replication in vivo. J. Virol. 74:2046–2051.
30. **Kyono, K., M. Miyashiro, and I. Taguchi.** 2002. Human eukaryotic initiation factor 4AII associates with hepatitis C virus NS5B protein *in vitro*. Biochem. Biophys. Res. Commun. 292:659–666.
31. **Lee, W. C., D. Zabetakis, and T. Melese.** 1992. NSR1 is required for pre-rRNA processing and for the proper maintenance of steady-state levels of ribosomal subunits. Mol. Cell. Biol. 12:3865–3871.
32. **Lindenbach, B. D., M. J. Evans, A. J. Syder, B. Wolk, T. L. Tellinghuisen, C. C. Liu, T. Maruyama, R. O. Hynes, D. R. Burton, J. A. McKeating, and C. M. Rice.** 2005. Complete replication of hepatitis C virus in cell culture. Science 309:623–626.
33. **Lindenbach, B. D., and C. M. Rice.** 2005. Unravelling hepatitis C virus replication from genome to function. Nature 436:933–938.
34. **Lohmann, V., F. Korner, U. Herian, and R. Bartenschlager.** 1997. Biochemical properties of hepatitis C virus NS5B RNA-dependent RNA polymerase and identification of amino acid sequence motifs essential for enzymatic activity. J. Virol. 71:8416–8428.
35. **Lohmann, V., F. Korner, J. Koch, U. Herian, L. Theilmann, and R. Bartenschlager.** 1999. Replication of subgenomic hepatitis C virus RNAs in a hepatoma cell line. Science 285:110–113.
36. **Ma, Y., T. Shimakami, H. Luo, N. Hayashi, and S. Murakami.** 2004. Mutational analysis of hepatitis C virus NS5B in the subgenomic replicon cell culture. J. Biol. Chem. 279:25474–25482.
37. **Matthews, D. A.** 2001. Adenovirus protein V induces redistribution of nucleolin and B23 from nucleolus to cytoplasm. J. Virol. 75:1031–1038.
38. **McBride, A. E., A. Schlegel, and K. Kirkegaard.** 1996. Human protein Sam68 relocalization and interaction with poliovirus RNA polymerase in infected cells. Proc. Natl. Acad. Sci. USA 93:2296–2301.
39. **Mottola, G., G. Cardinali, A. Ceccacci, C. Trozzi, L. Bartholomew, M. R. Torrisi, E. Pedrazzini, S. Bonatti, and G. Migliaccio.** 2002. Hepatitis C virus

nonstructural proteins are localized in a modified endoplasmic reticulum of cells expressing viral subgenomic replicons. Virology 293:31–43.
40. Murata, T., T. Ohshima, M. Yamaji, M. Husaka, Y. Miyanari, M. Hijikata, and K. Shimotohno. 2005. Suppression of hepatitis C virus replicon by TGF-beta. Virology 331:407–417.
41. Nisole, S., B. Krust, C. Callebaut, G. Guichard, S. Muller, J. P. Briand, and A. G. Hovanessian. 1999. The anti-HIV pseudopeptide HB-19 forms a complex with the cell-surface-expressed nucleolin independent of heparan sulfate proteoglycans. J. Biol. Chem. 274:27875–27884.
42. Nisole, S., B. Krust, E. Dam, A. Bianco, N. Seddiki, S. Loaec, C. Callebaut, G. Guichard, S. Muller, J. P. Briand, and A. G. Hovanessian. 2000. The HB-19 pseudopeptide 5[Kpsi(CH2N)PR]-TASP inhibits attachment of T lymphocyte- and macrophage-tropic HIV to permissive cells. AIDS Res. Hum. Retrovir. 16:237–249.
43. Nisole, S., B. Krust, and A. G. Hovanessian. 2002. Anchorage of HIV on permissive cells leads to coaggregation of viral particles with surface nucleolin at membrane raft microdomains. Exp. Cell Res. 276:155–173.
44. Nisole, S., E. A. Said, C. Mische, M. C. Prevost, B. Krust, P. Bouvet, A. Bianco, J. P. Briand, and A. G. Hovanessian. 2002. The anti-HIV pentameric pseudopeptide HB-19 binds the C-terminal end of nucleolin and prevents anchorage of virus particles in the plasma membrane of target cells. J. Biol. Chem. 277:20877–20886.
45. Osman, T. A., and K. W. Buck. 1997. The tobacco mosaic virus RNA polymerase complex contains a plant protein related to the RNA-binding subunit of yeast eIF-3. J. Virol. 71:6075–6082.
46. Piccininni, S., A. Varaklioti, M. Nardelli, B. Dave, K. D. Raney, and J. E. McCarthy. 2002. Modulation of the hepatitis C virus RNA-dependent RNA polymerase activity by the non-structural (NS) 3 helicase and the NS4B membrane protein. J. Biol. Chem. 277:45670–45679.
47. Pietschmann, T., V. Lohmann, G. Rutter, K. Kurpanek, and R. Bartenschlager. 2001. Characterization of cell lines carrying self-replicating hepatitis C virus RNAs. J. Virol. 75:1252–1264.
48. Qin, W., H. Luo, T. Nomura, N. Hayashi, T. Yamashita, and S. Murakami. 2002. Oligomeric interaction of hepatitis C virus NS5B is critical for catalytic activity of RNA-dependent RNA polymerase. J. Biol. Chem. 277:2132–2137.
49. Qin, W., T. Yamashita, Y. Shirota, Y. Lin, W. Wei, and S. Murakami. 2001. Mutational analysis of the structure and functions of hepatitis C virus RNA-dependent RNA polymerase. Hepatology 33:728–737.
50. Quadt, R., C. C. Kuo, K. S. Browning, R. P. Hershberger, and P. Ahlquist. 1993. Characterization of a host protein associated with brome mosaic virus RNA-dependent RNA polymerase. Proc. Natl. Acad. Sci. USA 90:1498–1502.
51. Randall, G., A. Grakoui, and C. M. Rice. 2003. Clearance of replicating hepatitis C virus replicon RNAs in cell culture by small interfering RNAs. Proc. Natl. Acad. Sci. USA 100:235–240.
52. Said, E. A., B. Krust, S. Nisole, J. Svab, J. P. Briand, and A. G. Hovanessian. 2002. The anti-HIV cytokine midkine binds the cell surface-expressed nucleolin as a low affinity receptor. J. Biol. Chem. 277:37492–37502.
53. Saito, I., T. Miyamura, A. Ohbayashi, H. Harada, T. Katayama, S. Kikuchi, Y. Watanabe, S. Koi, M. Onji, Y. Ohta, et al. 1990. Hepatitis C virus infection is associated with the development of hepatocellular carcinoma. Proc. Natl. Acad. Sci. USA 87:6547–6549.
54. Seeff, L. B. 1997. Natural history of hepatitis C. Hepatology 26:21S–28S.
55. Semenkovich, C. F., R. E. Ostlund, Jr., M. O. Olson, and J. W. Yang. 1990. A protein partially expressed on the surface of HepG2 cells that binds lipoproteins specifically is nucleolin. Biochemistry 29:9708–9713.
56. Shimakami, T., M. Hijikata, H. Luo, Y. Y. Ma, S. Kaneko, K. Shimotohno, and S. Murakami. 2004. Effect of interaction between hepatitis C virus NS5A and NS5B on hepatitis C virus RNA replication with the hepatitis C virus replicon. J. Virol. 78:2738–2748.
57. Shirota, Y., H. Luo, W. Qin, S. Kaneko, T. Yamashita, K. Kobayashi, and S. Murakami. 2002. Hepatitis C virus (HCV) NS5A binds RNA-dependent RNA polymerase (RdRP) NS5B and modulates RNA-dependent RNA polymerase activity. J. Biol. Chem. 277:11149–11155.
58. Sinclair, J. F., and A. D. O'Brien. 2002. Cell surface-localized nucleolin is a eukaryotic receptor for the adhesin intimin-gamma of enterohemorrhagic Escherichia coli O157:H7. J. Biol. Chem. 277:2876–2885.
59. Srivastava, M., and H. B. Pollard. 1999. Molecular dissection of nucleolin's role in growth and cell proliferation: new insights. FASEB J. 13:1911–1922.
60. Take, M., J. Tsutsui, H. Obama, M. Ozawa, T. Nakayama, I. Maruyama, T. Arima, and T. Muramatsu. 1994. Identification of nucleolin as a binding protein for midkine (MK) and heparin-binding growth associated molecule (HB-GAM). J. Biochem. (Tokyo) 116:1063–1068.
61. Tsukiyama-Kohara, K., N. Iizuka, M. Kohara, and A. Nomoto. 1992. Internal ribosome entry site within hepatitis C virus RNA. J. Virol. 66:1476–1483.
62. Tu, H., L. Gao, S. T. Shi, D. R. Taylor, T. Yang, A. K. Mircheff, Y. Wen, A. E. Gorbalenya, S. B. Hwang, and M. M. Lai. 1999. Hepatitis C virus RNA polymerase and NS5A complex with a SNARE-like protein. Virology 263: 30–41.
63. Wakita, T., T. Pietschmann, T. Kato, T. Date, M. Miyamoto, Z. Zhao, K. Murthy, A. Habermann, H. G. Krausslich, M. Mizokami, R. Bartenschlager, and T. J. Liang. 2005. Production of infectious hepatitis C virus in tissue culture from a cloned viral genome. Nat. Med. 11:791–796.
64. Wang, C., P. Sarnow, and A. Siddiqui. 1993. Translation of human hepatitis C virus RNA in cultured cells is mediated by an internal ribosome-binding mechanism. J. Virol. 67:3338–3344.
65. Wang, Q. M., M. A. Hockman, K. Staschke, R. B. Johnson, K. A. Case, J. Lu, S. Parsons, F. Zhang, R. Rathnachalam, K. Kirkegaard, and J. M. Colacino. 2002. Oligomerization and cooperative RNA synthesis activity of hepatitis C virus RNA-dependent RNA polymerase. J. Virol. 76:3865–3872.
66. Weiner, A. J., M. J. Brauer, J. Rosenblatt, K. H. Richman, J. Tung, K. Crawford, F. Bonino, G. Saracco, Q. L. Choo, M. Houghton, et al. 1991. Variable and hypervariable domains are found in the regions of HCV corresponding to the flavivirus envelope and NS1 proteins and the pestivirus envelope glycoproteins. Virology 180:842–848.
67. Weiner, A. J., H. M. Geysen, C. Christopherson, J. E. Hall, T. J. Mason, G. Saracco, F. Bonino, K. Crawford, C. D. Marion, K. A. Crawford, et al. 1992. Evidence for immune selection of hepatitis C virus (HCV) putative envelope glycoprotein variants: potential role in chronic HCV infections. Proc. Natl. Acad. Sci. USA 89:3468–3472.
68. Yamashita, T., S. Kaneko, Y. Shirota, W. Qin, T. Nomura, K. Kobayashi, and S. Murakami. 1998. RNA-dependent RNA polymerase activity of the soluble recombinant hepatitis C virus NS5B protein truncated at the C-terminal region. J. Biol. Chem. 273:15479–15486.
69. Yanagi, M., M. St. Claire, S. U. Emerson, R. H. Purcell, and J. Bukh. 1999. *In vivo* analysis of the 3' untranslated region of the hepatitis C virus after *in vitro* mutagenesis of an infectious cDNA clone. Proc. Natl. Acad. Sci. USA 96:2291–2295.
70. Yang, T. H., W. H. Tsai, Y. M. Lee, H. Y. Lei, M. Y. Lai, D. S. Chen, N. H. Yeh, and S. C. Lee. 1994. Purification and characterization of nucleolin and its identification as a transcription repressor. Mol. Cell. Biol. 14:6068–6074.
71. Yi, M., and S. M. Lemon. 2003. 3' nontranslated RNA signals required for replication of hepatitis C virus RNA. J. Virol. 77:3557–3568.
72. Zhong, J., P. Gastaminza, G. Cheng, S. Kapadia, T. Kato, D. R. Burton, S. F. Wieland, S. L. Uprichard, T. Wakita, and F. V. Chisari. 2005. Robust hepatitis C virus infection *in vitro*. Proc. Natl. Acad. Sci. USA 102:9294–9299.

Maintenance of self-renewal ability of mouse embryonic stem cells in the absence of DNA methyltransferases Dnmt1, Dnmt3a and Dnmt3b

Akiko Tsumura[1,4], Tomohiro Hayakawa[2], Yuichi Kumaki[3,6], Shin-ichiro Takebayashi[1], Morito Sakaue[1], Chisa Matsuoka[1], Kunitada Shimotohno[4], Fuyuki Ishikawa[5], En Li[7], Hiroki R. Ueda[3], Jun-ichi Nakayama[2] and Masaki Okano[1,*]

[1]*Laboratory for Mammalian Epigenetic Studies,* [2]*Laboratory for Chromatin Dynamics, and* [3]*Laboratory for Systems Biology, Center for Developmental Biology, RIKEN, 2-2-3 Minatojima-Minamimachi, Chuo-ku, Kobe 650-0047, Japan*

[4]*Department of Viral Oncology, Institute for Virus Research, Kyoto University, 53 Kawaharacho, Shogoin, Sakyo-ku, Kyoto 606-8501, Japan*

[5]*Department of Gene Mechanisms, Graduate School of Biostudies, Kyoto University, Kitashirakawa-Oiwake-cho, Sakyo-ku, Kyoto 606-8502, Japan*

[6]*INTEC Web and Genome Informatics Corp., 1-3-3 Shinsuna, Koto-ku, Tokyo 136-8637, Japan*

[7]*Epigenetics Program, Novartis Institute for Biomedical Research, 250 Massachusetts Ave., Cambridge, MA 02139, USA*

DNA methyltransferases Dnmt1, Dnmt3a and Dnmt3b cooperatively regulate cytosine methylation in CpG dinucleotides in mammalian genomes, providing an epigenetic basis for gene silencing and maintenance of genome integrity. Proper CpG methylation is required for the normal growth of various somatic cell types, indicating its essential role in the basic cellular function of mammalian cells. Previous studies using *Dnmt1*$^{-/-}$ or *Dnmt3a*$^{-/-}$*Dnmt3b*$^{-/-}$ ES cells, however, have shown that undifferentiated embryonic stem (ES) cells can tolerate hypomethylation for their proliferation. In an attempt to investigate the effects of the complete loss of CpG DNA methyltransferase function, we established mouse ES cells lacking all three of these enzymes by gene targeting. Despite the absence of CpG methylation, as demonstrated by genome-wide methylation analysis, these triple knockout (TKO) ES cells grew robustly and maintained their undifferentiated characteristics. TKO ES cells retained pericentromeric heterochromatin domains marked with methylation at Lys9 of histone H3 and heterochromatin protein-1, and maintained their normal chromosome numbers. Our results indicate that ES cells can maintain stem cell properties and chromosomal stability in the absence of CpG methylation and CpG DNA methyltransferases.

Introduction

Vertebrate genomes are methylated on cytosines at levels much higher than those of other eukaryotic organisms, and are almost exclusively methylated at CpG dinucleotides (Bird 2002). CpG methylation plays an important role in epigenetic gene silencing and maintenance of genome stability, and is involved in a broad range of physiological and pathological processes in mammals, including embryogenesis, genome imprinting and tumorigenesis (Jones & Baylin 2002; Li 2002; Robertson 2005). In mice, three CpG DNA methyltransferases, Dnmt1, Dnmt3a and Dnmt3b, coordinately regulate CpG methylation in the genome (Li *et al.* 1992; Okano *et al.* 1999). Reduction of CpG methylation by inactivating these enzymes or related molecules in various mammalian cells results in growth defects, cell death, activation of retrotransposons and genome instability (Walsh *et al.* 1998; Xu *et al.* 1999; Jackson-Grusby *et al.* 2001; Rhee *et al.* 2002; Eden *et al.* 2003; Gaudet *et al.* 2003; Bourc'his & Bestor 2004; Dodge *et al.* 2005; Hata *et al.* 2006), indicating that CpG methylation plays a fundamental role in basic cellular functions of mammalian cells. Unlike differentiated somatic cells, undifferentiated ES cells can tolerate hypomethylation caused by inactivation of Dnmt1 or inactivation of both

Communicated by: Fumio Hanaoka
**Correspondence*: E-mail: okano@cdb.riken.jp

DOI: 10.1111/j.1365-2443.2006.00984.x

Dnmt3a and Dnmt3b for their proliferation (Lei *et al.* 1996; Chen *et al.* 2003; Jackson *et al.* 2004), indicating that gene silencing and chromatin structures are regulated differently in ES cells.

Post-translational modifications of specific amino acid residues of histones are also important for chromatin dynamics and epigenetic gene regulation (Jenuwein & Allis 2001). Functional relationships between CpG methylation and histone modification have been demonstrated in several species (Tamaru & Selker 2001; Jackson *et al.* 2002; Lehnertz *et al.* 2003; Tariq *et al.* 2003; Vire *et al.* 2006). Biochemical analyses have also shown that methyl-CpG-binding proteins interact with either histone deacetylases or histone methyltransferases (Jones *et al.* 1998; Nan *et al.* 1998; Ng *et al.* 1999; Wade *et al.* 1999; Zhang *et al.* 1999; Fujita *et al.* 2003; Sarraf & Stancheva 2004), further supporting the mechanistic links between these epigenetic mechanisms. Interestingly, a previous study using *Dnmt1*$^{-/-}$ and *Dnmt3a*$^{-/-}$*Dnmt3b*$^{-/-}$ ES cells showed that ES cells with a reduced level of CpG methylation maintain proper localization of the repressive chromatin markers histone H3 methylated at lysine 9 (H3K9) and heterochromatin protein-1 (HP1) at pericentromeric heterochromatin (Lehnertz *et al.* 2003), indicating that CpG methylation may contribute little to the regulation of higher-order chromatin structures in ES cells. That study, however, remains inconclusive because the mutant ES cells had residual CpG methylation and functional CpG methyltransferase activity.

In this study, we address whether mouse ES cells can survive in the absence of epigenetic regulation by CpG methylation, and if so, whether higher-order chromatin structures can be maintained in these cells. We established ES cells deficient for all three CpG methyltransferases, Dnmt1, Dnmt3a and Dnmt3b. We show that ES cells without CpG methylation maintain stem cell properties, proliferation ability, heterochromatic domains marked with H3K9 trimethylation, and euploidy.

Results

Establishment of Dnmt1/Dnmt3a/Dnmt3b triple knockout ES cells

We investigated the effects of the complete loss of CpG DNA methyltransferase function by inactivating *Dnmt1* via two rounds of gene targeting in *Dnmt3a*$^{-/-}$*Dnmt3b*$^{-/-}$ ES cells (Fig. 1A). This procedure yielded five independent clones of viable TKO *Dnmt1*$^{-/-}$*Dnmt3a*$^{-/-}$*Dnmt3b*$^{-/-}$ ES cells. We confirmed the accuracy of the gene targeting in these five cell lines by Southern blotting analysis (Fig. 1B and data not shown). Three of the five TKO cell lines were characterized in detail by Western blotting and RT-PCR analyses, showing the loss of gene products (Fig. 1B–D), and we used these for further studies.

Absence of CpG methylation in TKO ES cells

We evaluated the status of genome-wide CpG methylation in the TKO cells by several independent methods. We first examined CpG methylation of repetitive sequences by Southern hybridization using methylation-sensitive restriction enzymes. The methylation of two widely dispersed retroelement sequences, C-type endogenous retrovirus and intracisternal-A particles (IAP), was much lower in TKO cells as compared with *Dnmt1*$^{-/-}$ cells or *Dnmt1*$^{+/-}$*Dnmt3a*$^{-/-}$*Dnmt3b*$^{-/-}$ clones (Fig. 2A). In TKO cells, the digest patterns for CpG methylation-sensitive *Hpa*II and its CpG methylation-insensitive isoschizomer *Msp*I were indistinguishable, suggesting that CpG methylation in TKO cells was below the detection limit (Fig. 2A). Analysis of minor satellite repeats at centromeric regions and major satellite repeats at pericentromeric regions showed similarly reduced CpG methylation states in TKO cells (Fig. 2A).

We next examined the profiles and amounts of CpG methylation in TKO cells using bisulfite sequencing analysis, which can determine the exact sites of methylcytosine (Clark *et al.* 1994). Pericentromeric major satellite repeats, retroelement repeats, and the single-copy imprinted genes *Snrpn* and *Igf2r* all showed extensive loss of CpG methylation (Fig. 2B). We also sequenced random fragments of bisulfite-treated genomic DNA via shotgun sequencing and compared the sequences to the mouse genome (Table 1 and <http://www.dbsb.org/>). Two experiments using TKO cells showed that almost all methylcytosines were lost in 786 CpG sites over about 75 kb (Table 1). We detected a very small amount of methylcytosine-signals both at CpG sites (0.4%) and non-CpG sites (0.1–0.4%), possibly reflecting residual methylcytosines in the genome of TKO cells resulting from mechanisms other than methylation by Dnmt1/Dnmt3a/Dnmt3b. Such low levels, however, are nearly equivalent to the low frequency of experimental errors, including nucleotide misincorporation by Taq polymerase or incomplete bisulfite conversion. These data suggest that both CpG and non-CpG methylation in the TKO cells were below the limit of accuracy in our experimental procedures.

We then investigated the loss of CpG methylation at the cellular level by focusing on two cellular responses, localization of a methyl-CpG-binding protein and silencing of retroelements. To visualize the cytological distribution

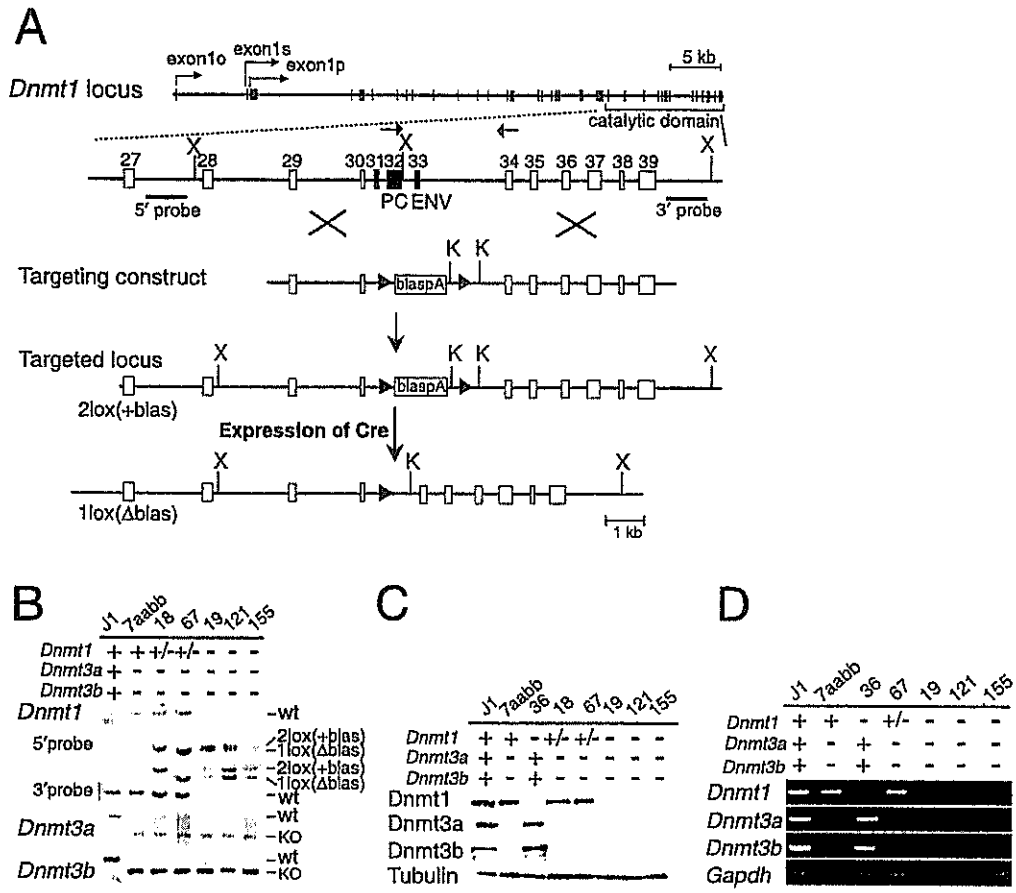

Figure 1 Generation of Dnmt1$^{-/-}$Dnmt3a$^{-/-}$Dnmt3b$^{-/-}$ ES cells. (A) Targeting of *Dnmt1* in *Dnmt3a*$^{-/-}$*Dnmt3b*$^{-/-}$ ES cells. To create a null allele, exons 31–33, encoding highly conserved Pro-Cys (PC) and Glu-Asn-Val (ENV) motifs, were replaced with the blasticidin resistance gene flanked with *loxP* sites (2lox(+blas)). Introduction of Cre excised the blasticidin resistance gene (1lox(Δblas)). The horizontal lines labeled "5′ probe" and "3′ probe" represent the two probes used for Southern blot analyses, and the arrows represent the primers used in the RT-PCR analysis. X, *Xba*I; K, *Kpn*I. (B–D) J1, wild-type line; 7aabb, *Dnmt3a*$^{-/-}$*Dnmt3b*$^{-/-}$ ES cell line; 36, a *Dnmt1*$^{-/-}$ ES cell line; 18 and 67, *Dnmt1*$^{+/-}$*Dnmt3a*$^{-/-}$*Dnmt3b*$^{-/-}$ parental lines of TKO ES cells with or without excision of the blasticidin gene by Cre (18, 2lox(+blas); 67, 1lox(Δblas)); 19, 121 and 155, independent *Dnmt1*$^{-/-}$*Dnmt3a*$^{-/-}$*Dnmt3b*$^{-/-}$ TKO lines. (B) Southern blot analysis of the mutant cell lines. Genomic DNA was digested with *Kpn*I (*Dnmt1*-5′probe), *Xba*I (*Dnmt1*-3′probe), *Hin*dIII (*Dnmt3a* probe) or *Bam*HI (*Dnmt3b* probe). wt, wild-type alleles; KO, mutant alleles; 2lox(+blas) and 1lox(Δblas), targeted *Dnmt1* alleles. (C) Western blot analysis of the mutant cell lines with anti-Dnmt1, anti-Dnmt3a or anti-Dnmt3b. Anti-tubulin was used as a control for equal protein loading. (D) RT-PCR analysis of the mutant cell lines with primers for *Dnmt1*, *Dnmt3a*, and *Dnmt3b*. Glyceraldehyde 3-phosphate dehydrogenase (*Gapdh*) was used as a control for equal RNA loading.

of CpG methylation in ES cells, we introduced and expressed green fluorescent protein fused to the methyl-CpG binding domain of MBD1 (GFP-MBD, Fujita *et al.* 1999). In interphase nuclei of wild-type and *Dnmt1*$^{-/-}$ ES cells, GFP-MBD mainly localized to pericentromeric heterochromatin regions that were densely stained by 4′,6′-diamino-2-phenylindole (DAPI). In contrast, GFP-MBD distribution was diffuse in TKO cell nuclei, and its localization was not restricted to pericentromeric heterochromatin (Fig. 2C), in agreement with our observation of extensive loss of CpG methylation at pericentromeric regions in these cells (Fig. 2A,B). We also examined the expression of two retroelements, IAP and LINE1, which are normally silenced and are de-repressed in severely hypomethylated embryos or germ cells (Walsh *et al.* 1998; Bourc'his & Bestor 2004; Hata *et al.* 2006). Consistent with the CpG methylation status of these retroelements (Fig. 2B), transcripts of

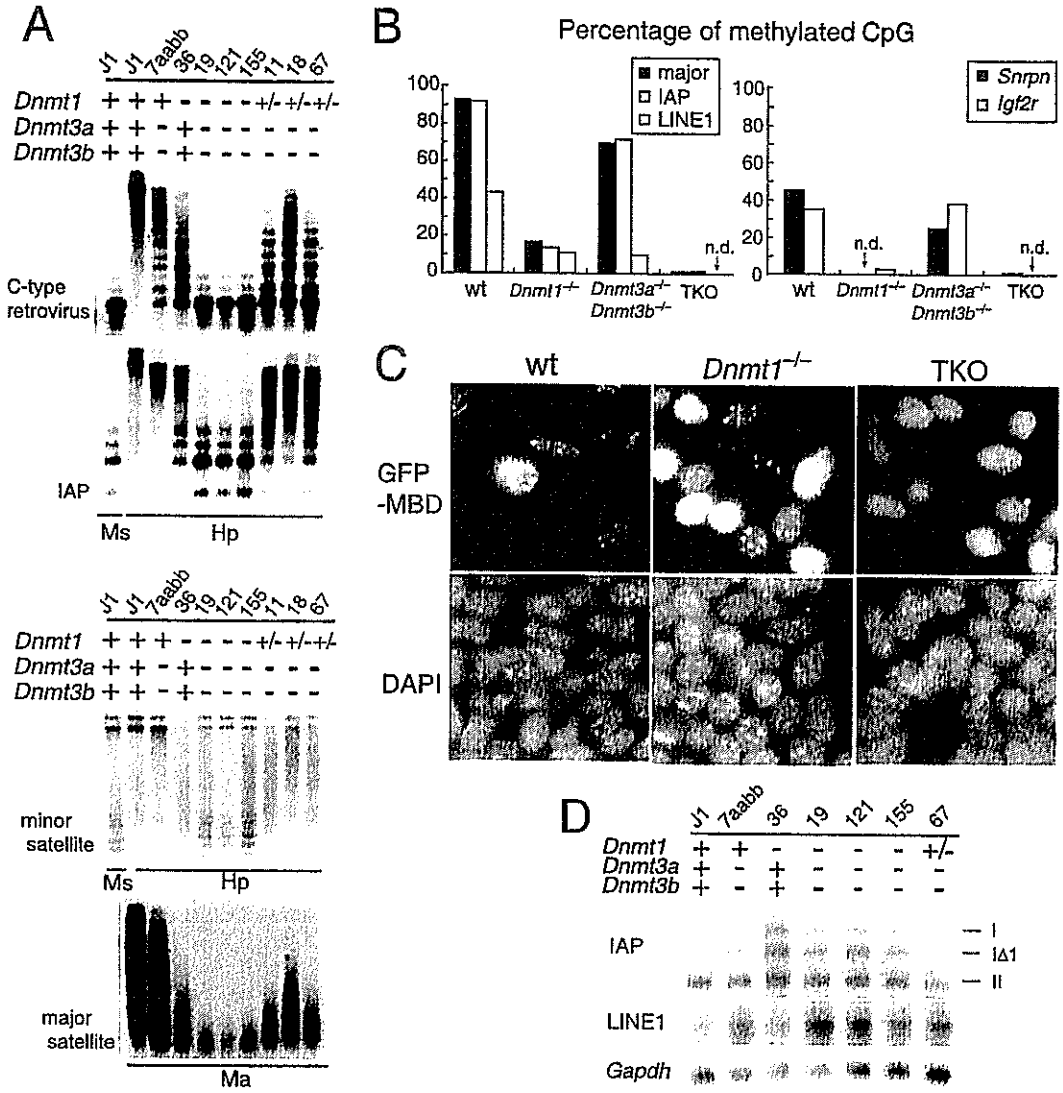

Figure 2 Extensive loss of CpG methylation in TKO cells. (A) DNA methylation of repetitive sequences as determined by Southern analysis of TKO cells. Genomic DNA was digested with CpG methylation–sensitive *Hpa*II (Hp) and *Mae*I (Ma) or CpG methylation–insensitive *Msp*I (Ms) and analyzed with probes against the following: C-type endogenous retrovirus, intracisternal-A particle retroelements (IAP), centromeric repeats (minor satellites), and pericentromeric repeats (major satellites). Clone 11 was a non-targeted clone during the second round of targeting of *Dnmt1*, which retained an intact *Dnmt1* allele and underwent the same number of passages as TKO cells. (B) DNA methylation analysis of repetitive sequences (pericentromeric major satellite repeats, IAP and LINE1; left) and imprinted genes (*Snrpn* and *Igf2r*; right) by bisulfite sequencing analysis. The percentages of methylcytosine signal out of total CpG sites analyzed in the sequenced clones are indicated. n.d., not detected. (C) Localization of GFP-MBD in interphase nuclei of ES cells. DNA was visualized by DAPI. (D) Northern blot analysis of poly(A)$^+$ RNA from the various ES cell lines using IAP and LINE1 probes. I and IΔ1, full-length transcripts and variant truncated transcripts of type I IAP; II, type II IAP.

IAP were elevated in both the TKO and the *Dnmt1*$^{-/-}$ ES cells, whereas transcripts of LINE1 were elevated mainly in TKO cells (Fig. 2D). These data are consistent with the absence of CpG methylation in the TKO cells.

Maintenance of stem cell properties in TKO ES cells

Despite the absence of CpG methylation, TKO cells retained the morphological features of undifferentiated

Table 1 Random bisulfite sequencing analysis. Random fragments of bisulfite-treated genomic DNA from the ES cell lines were sequenced, and the methylation status of each cytosine was determined by alignment with the mouse genome. Methylation status of clones that mapped to multiple loci in the mouse genome was based on the highest probability alignment with the genomic sequence.

	No. of clones	Total (bp)	No. of methylcytosines/total no. of sites			
			CpG	CpA	CpC	CpT
Wild-type	119	16327	112/136 (82%)	7/1117	3/779	6/1142
Dnmt3a$^{-/-}$*3b*$^{-/-}$	63	8541	11/72 (15%)	3/661	5/415	3/588
Dnmt1$^{-/-}$	112	15450	26/143 (18%)	8/1106	2/765	1/1057
TKO (#19)	383	57404	*2/559 (0.4%)	8/4125	11/2725	5/4011
TKO (#121)	127	17448	*1/227 (0.4%)	3/1296	4/1009	1/1201

*Three cytosines at CpG sites remained unconverted to uracil after the bisulfite reaction in the TKO cells, and two of the three cytosines were derived from clones that contained more than three unconverted cytosines at non-CpG sites. In these cases, all unconverted cytosines were clustered within a 20-bp palindromic sequence, indicating the possibility of incomplete conversion by the bisulfite reaction.

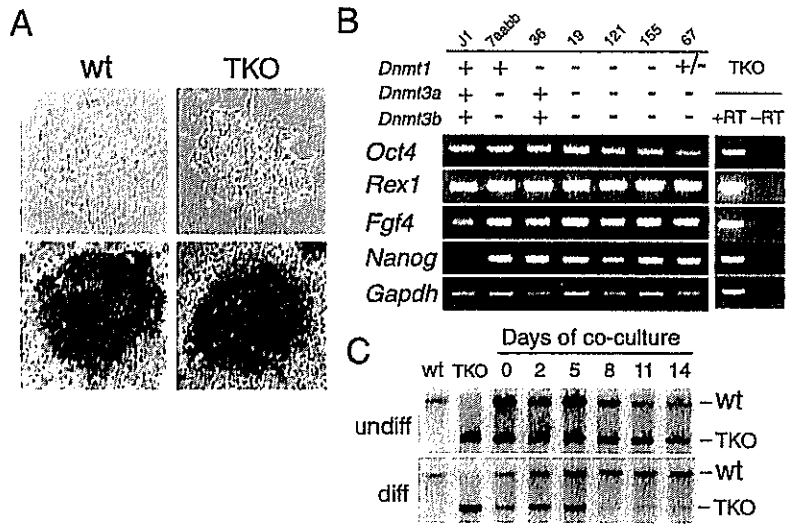

Figure 3 Maintenance of undifferentiated features in TKO cells. (A) Phase-contrast microscopic images (top) and alkaline phosphatase staining (bottom) of wild-type (wt) and TKO cells. (B) RT-PCR analysis of four representative undifferentiated ES cell markers, *Oct4*, *Rex1*, *Fgf4* and *Nanog*. No signal was observed in the negative control lacking reverse transcriptase (RT). (C) Growth competition in a mixture of wt and TKO cells under culture conditions that maintain the undifferentiated state (undiff, top) or promote differentiation (diff, bottom). Changes in the fraction of wild-type and TKO cells in the cell population at the indicated days were determined by Southern analysis using the *Dnmt3b* probe.

ES cells and stained positive for alkaline phosphatase activity, indicative of a pluripotent, undifferentiated state (Fig. 3A). TKO cells also expressed four other typical markers of undifferentiated cells (Oct4, Rex1, Fgf4 and Nanog) at the same or higher levels than wild-type ES cells (Fig. 3B). Growth curve experiments suggest that proliferation of undifferentiated TKO cells was comparable to, although slightly slower than, that of wild-type ES cells (Supplementary Fig. S1). We also estimated the growth rate of TKO cells by growth competition analysis, in which wild-type and TKO cells were cocultured, and the change in the fraction of wild-type and TKO cells in the cell population during the culture period was determined by Southern hybridization. The growth of undifferentiated TKO cells was comparable to that of wild-type cells, whereas their growth was delayed upon differentiation by formation of embryoid bodies (Fig. 3C), consistent with previous findings using *Dnmt1*$^{-/-}$ ES cells (Lei *et al.* 1996). These results suggest that CpG methylation is not essential for the self-renewal of ES cells in an undifferentiated state.

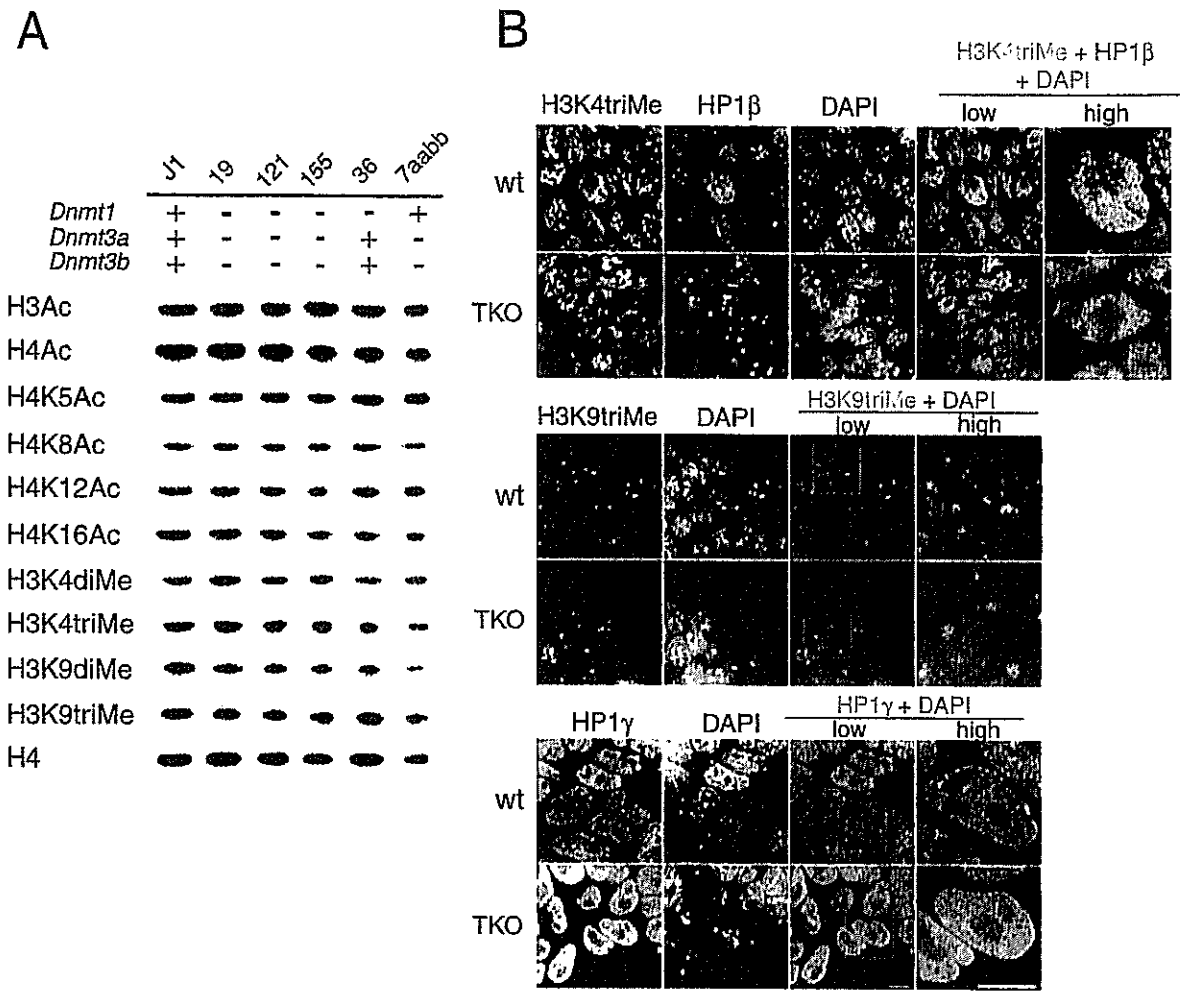

Figure 4 Maintenance of global chromatin structure in TKO cells. (A) Western blot analysis of global histone acetylation and methylation levels. H3Ac, acetylated histone H3; H4Ac, acetylated histone H4; H4K5Ac, H4K8Ac, H4K12Ac and H4K16Ac, acetylation at Lys5, Lys8, Lys12, or Lys16 of histone H4, respectively; H3K4diMe and H3K9diMe, dimethylation at Lys4 or Lys9 of histone H3, respectively; H3K4triMe and H3K9triMe, trimethylation at Lys4 or Lys9 of histone H3, respectively; H4, histone H4. Anti-histone H4 was used as a loading control. (B) Immunofluorescence analysis of interphase chromatin from wild-type (wt) and TKO cells using antibodies against trimethylated H3K9, trimethylated H3K4, HP1-β and HP1-γ. DNA was visualized with DAPI. Merged images represent overlays of immunofluorescence signal (green or red) and DAPI (blue) as indicated. "Low" and "high" indicate low and high magnification, respectively.

Maintenance of global chromatin structures in TKO ES cells

We next examined whether the absence of CpG methylation affects the post-translational modification of histone termini in ES cells. We assessed global histone acetylation and methylation by Western blotting using modification- and site-specific antibodies against histones H3 and H4. Acetylation at lysines of histones H3 and H4 and methylation at Lys4 of histone H3 (H3K4) are generally associated with transcriptionally active chromatin, whereas methylation at Lys9 of histone H3 (H3K9) is associated with transcriptionally repressed chromatin. Overall, the amounts of histone acetylation and methylation in TKO cells at most sites detected by the antibodies were similar to those in wild-type cells (Fig. 4A). We did not detect a significant increase in the acetylation of histone H4 at Lys5 in TKO cells, which was observed in *Dnmt3a*$^{-/-}$ *Dnmt3b*$^{-/-}$ ES cells of high passage numbers (Jackson *et al.* 2004).

We also investigated whether the absence of CpG methylation affects higher-order chromatin structure in ES cells. Trimethylation of H3K9 and co-localization of HP1 are characteristic features of pericentromeric heterochromatin, whereas methylation of H3K4 is normally absent in this region (Lehnertz *et al.* 2003; Maison & Almouzni 2004). Immunofluorescence analysis of TKO cells showed that the focal staining patterns of trimethylated H3K9 and HP1 overlapped with DAPI-dense heterochromatin regions, similar to the results for wild-type cells (Fig. 4B). The diffuse speckled patterns of trimethylated H3K4 found in TKO cell nuclei were also indistinguishable from those of wild-type cells (Fig. 4B). We did not observe a redistribution of H3K4 methylation to pericentromeric heterochromatin in TKO cells, as observed in hypomethylated mouse fibroblasts deficient for *Lsh* (Yan *et al.* 2003), a member of the SNF/helicase family involved in the control of global CpG methylation. Furthermore, analysis of metaphase chromosomes showed that TKO cells retained normal chromosomal number and banding patterns (Supplementary Fig. S2 and data not shown), indicating that condensation and segregation of chromosomes during mitosis occur properly in the absence of CpG methylation in ES cells.

Discussion

We have established the first mammalian cells deficient for the three known CpG DNA methyltransferases; CpG methylation is apparently absent in these cells. Our results provide direct genetic evidence that CpG methylation is dispensable for ES cell growth in an undifferentiated state, as suggested previously (Lei *et al.* 1996; Chen *et al.* 2003; Jackson *et al.* 2004). This stands in clear contrast to cases involving other cell types. Loss of *Dnmt1* in mouse embryonic fibroblasts leads to growth arrest associated with increased expression of *p21Waf1/Cip1* and *p57Kip2*, and *p53*-dependent cell death (Jackson-Grusby *et al.* 2001); moreover, the loss of both *DNMT1* and *DNMT3B* in human colon cancer cell lines causes growth impairment that is dependent on re-expression of *p16INK4A* (Rhee *et al.* 2002; Bachman *et al.* 2003). The unique cell cycle regulation of mouse ES cells (Hong & Stambrook 2004) may explain the robust growth and viability of our TKO cells.

Reduction of Dnmt1 activity in mice has been shown to induce tumors and chromosomal instability (Eden *et al.* 2003; Gaudet *et al.* 2003), and global hypomethylation in male germ cells results in meiotic abnormality (Bourc'his & Bestor 2004; Hata *et al.* 2006). Furthermore, inactivation of Dnmt3b in primary mouse embryonic fibroblast cells causes aneuploidy and chromosomal breaks and fusions (Dodge *et al.* 2005). These results suggest that proper CpG methylation level is important for chromosomal stability, at least in certain cell types. It remains unknown why undifferentiated ES cells retain chromosomal stability without CpG methylation and CpG DNA methyltransferases. One possibility is that ES cells maintain stable heterochromatin and chromosomes by an epigenetic mechanism that is independent of CpG methylation. Previous studies have shown that ES cells have both unique global chromatin modifications and heterochromatin arrangement, and that chromatin proteins bind more loosely to chromatin in ES cells than in differentiated cells, indicating the existence of specific epigenetic regulatory mechanisms in ES cells (Kimura *et al.* 2004; Meshorer *et al.* 2006). The absence or reduction of such mechanisms may be attributed to the chromosomal abnormality in differentiated cell types with decreased levels of CpG methylation. Taken together, these results suggest that the relative contribution of CpG methylation to both chromosomal stability and epigenetic gene silencing varies in a cell type-specific manner.

Our results suggest that at least some functional properties of heterochromatic domains are retained in the absence of CpG methylation in ES cells. However, it is possible that some unrecognized changes in heterochromatin occur in TKO cells. Indeed, the redistribution of the histone variant macroH2A into pericentromeric heterochromatin in hypomethylated *Dnmt1*$^{-/-}$ ES cells has recently been reported (Ma *et al.* 2005), indicating that CpG methylation modulates some properties of heterochromatic domains. Although the apparent contribution of CpG methylation to the steady-state heterochromatin structure in ES cells may be small, it is possible that CpG methylation might serve as a mark for anchoring heterochromatin during dynamic chromatin remodeling or during multiple replication processes. Further studies in this line are required for understanding the exact role of CpG methylation in higher-order chromatin structures.

The genomes of primordial germ cells and preimplantation embryos are extensively hypomethylated during normal embryogenesis (Hajkova *et al.* 2002; Li 2002), and global reduction of CpG methylation is a common feature of neoplasia (Feinberg *et al.* 2006). The generation of these triple methyltransferase-deficient ES cells will be useful in studying the role of CpG methylation in cell type-specific epigenetic regulation during normal and pathological processes. These cells will be also useful in investigating the function of chromatin modifications and remodeling in the absence of CpG methylation and endogenous CpG DNA methyltransferases in mammalian cellular conditions.

Experimental procedures

ES cell culture

ES cells were maintained in Glasgow modified Eagle medium (Sigma) supplemented with 15% foetal bovine serum, 0.1 mM nonessential amino acids (Invitrogen), 1 mM sodium pyruvate, 0.1 mM 2-mercaptoethanol and 2000 U/mL of leukemia inhibitory factor (LIF) and were grown on gelatinized culture dishes without feeder cells. For growth curve experiments, 0.9×10^5 ES cells were plated on gelatinized 10-cm culture dishes on the first day. Then, ES cells were passaged every 2 days with 6- to 12-fold dilution. For induction of differentiation by embryoid body formation, ES cells were seeded on low cell-binding dishes (Nunc) in medium without LIF. For growth competition analysis, wild-type and TKO cells were mixed at a 1 : 1 ratio and cultured either as undifferentiated ES cells or as embryoid bodies, as previously described (Lei *et al.* 1996). The change in cell population between wild-type and TKO cells was determined by Southern analysis using the *Dnmt3b* probe, which distinguishes between wild-type and TKO cells.

Generation of Dnmt1$^{-/-}$Dnmt3a$^{-/-}$Dnmt3b$^{-/-}$ ES cells

The following nucleotide positions of *Dnmt1* genomic DNA all refer to AC073775.2. The *Dnmt1* targeting vector, pTA009, was constructed by subcloning the 3-kb 5' arm (nt 66903–70025) and the 4-kb 3' arm (nt 71625–76570) of *Dnmt1* genomic DNA and a splicing acceptor–internal ribosomal entry site–blasticidin resistant gene cassette flanked by *loxP* sites (*loxP*-SAiresBlas-*loxP*) into pBluescript II SK. The *Dnmt1* genomic fragments were amplified by PCR from genomic DNA of ES cells (Supplementary Table S1). For targeting of the first *Dnmt1* allele, the *Dnmt1* targeting vector was transfected in *Dnmt3a*$^{-/-}$*Dnmt3b*$^{-/-}$ ES cells (Okano *et al.* 1999) via electroporation, and transfected cells were selected with 5 μg/mL blasticidin. Drug-resistant clones were screened by Southern hybridization using a 5' probe (nt 65650–66729) and a 3' probe (nt 76647–77192) external to the targeting construct (Fig. 1A). The targeting frequency was 14% (3/22). To generate blasticidin-sensitive ES cells, Cre recombinase was transiently expressed in blasticidin-resistant *Dnmt1*$^{+/-}$*Dnmt3a*$^{-/-}$*Dnmt3b*$^{-/-}$ ES cells (clone 18) by lipofection of a circular Cre expression plasmid. For targeting of the second wild-type Dnmt1 allele, the same targeting vector was transfected into blasticidin-sensitive *Dnmt1*$^{+/-}$*Dnmt3a*$^{-/-}$*Dnmt3b*$^{-/-}$ ES cells (clone 67), and the transfected cells were selected with 3.5 μg/mL blasticidin. Targeting frequency was 4% (5/113).

DNA methylation analysis

For Southern analysis, genomic DNA was digested with the CpG methylation-sensitive restriction enzymes *Hpa*II or *Mae*II (Roche), blotted and hybridized with probes specific for C-type endogenous retroviruses (pMO), IAP, minor satellite repeats, or major satellite repeats (Okano *et al.* 1999). For bisulfite sequencing analysis of specific sequences, 2 μg of genomic DNA digested with *Hin*dIII was treated with bisulfite followed by deamination (Clark *et al.* 1994). Deaminated fragments were amplified with primers for IAP, LINE1, major satellite repeats, *Igf2r* or *Snrpn* (Supplementary Table S1). We sequenced 15–30 clones for repetitive sequences and 9–15 clones for single-copy genes. Bisulfite sequencing of random genomic fragments was carried out as previously described (Ramsahoye *et al.* 2000). The sequences were aligned to the mouse genome sequence, NCBI Mouse Build 33 (Y.K. and H.R.U., unpublished data). Sequenced clones containing five non-CpG cytosines per sequenced clone that remained unconverted to uracil by the bisulfite reaction were excluded from the analysis. Overall, 80% of the sequenced clones longer than 51 bp could be mapped to the mouse genome. For localization of the methyl-CpG-binding protein, the GFP-MBD1(MBD+NLS) plasmid, which encodes an enhanced green fluorescent protein (EGFP) fused to the amino terminus of human MBD1 containing both a methyl-CpG-binding domain and a nuclear localization signal (Fujita *et al.* 1999; gift from M. Nakao), was transfected into the ES cells by Lipofectamine (Invitrogen). After 16 h of culture, the transfected cells were fixed with 4% paraformaldehyde and 0.5% [v/v] Triton X-100 in phosphate buffered saline (PBS) and were stained with DAPI.

RT-PCR and Northern blotting

RNA samples were isolated from subconfluent cells using the Trizol RNA extraction reagent (Invitrogen). Primer sets for *Dnmt1*, *Dnmt3a*, *Dnmt3b*, *Oct3/4*, *Rex1*, *Nanog*, *Fgf4* and *Gapdh* were used for RT-PCR (Supplementary Table S1). Poly(A)$^+$ RNA was prepared using the Poly(A) Tract purification system (Promega). Poly(A)$^+$ RNA (1 μg) was used for Northern analysis. The LINE1 probe was amplified by PCR (Supplementary Table S1).

Antibodies, Western blotting and immunofluorescence analysis

The following antibodies were used: anti-Dnmt1 (sc-20701) and anti-[acetyl-Lys5]H4 (sc8659-R) from Santa Cruz Biotechnology; anti-Dnmt3a (IMG-268) and anti-Dnmt3b (IMG-184) from IMGENEX; anti-α-tubulin (CP06) from Oncogene; anti-acetylated histone H3 (Lys9, Lys14; 06–599), anti-acetylated histone H4 (Lys5, Lys8, Lys12, Lys16; 06–866), anti-[acetyl-Lys8]H4 (17-211), anti-[acetyl-Lys12]H4 (17-211), anti-[acetyl-Lys16]H4 (06-762 and 07-329), anti-[dimethyl-Lys4]H3 (07–030), anti-[dimethyl-Lys9]H3 (07-212) and anti-histone H3 (06-755) from Upstate; anti-[acetyl-Lys16]H4 (ab1762), anti-[trimethyl-Lys4]H3 (ab8580) and anti-[trimethyl-Lys9]H3 (ab8898) from Abcam; and anti-HP1β (1MOD 1A9) and anti-HP1γ (2MOD 1G6) from EUROMEDEX. Alexa 488- and Alexa 546-conjugated secondary antibodies were purchased from Molecular Probes. A polyclonal antibody for Dnmt1 was raised against a modified linear peptide, CRESASAAVKAKEEAATKD, corresponding to the carboxy terminus of mouse Dnmt1. For Western blot analysis, whole-cell extracts were prepared by sonication in SDS-PAGE sample buffer, fractionated on an 8% SDS-PAGE gel and blotted using standard

procedures. Histones from ES cell nuclei were extracted with 0.2 mol/L H_2SO_4, precipitated with trichloroacetic acid (final concentration 25%), fractionated on an 18% SDS-PAGE gel and blotted in 10 mM CAPS (pH 11.0)/20% methanol. Indirect immunofluorescence staining was performed essentially as described (Lehnertz *et al.* 2003), with some modifications as follows. Wild-type and knockout ES cells were cultured in 35-mm glass-bottom dishes (MatTek) precoated with 0.2% gelatin in PBS. The cells were fixed with 2% formaldehyde in PBS, permeabilized with 0.1% sodium citrate containing 0.1% [v/v] Triton X-100 followed by incubation in blocking buffer (PBS, 2.5% BSA, 0.1% [v/v] Tween-20, 10% fetal bovine serum). Primary antibodies (diluted in blocking buffer) were added to fixed cells. After washing with PBS, 0.25% BSA, 0.1% [v/v] Tween-20, cells were re-fixed with 2% formaldehyde in PBS and then incubated with secondary antibody. After several washes with PBS, 0.1% [v/v] Tween-20, the stained cells were processed sequentially with 20%, 40%, 60% and 80% [v/v] glycerol in PBS containing 2.5% 1,4-diazobicyclo-(2,2,2)-octane (DABCO) for mounting. The 20% and 40% glycerol contained 0.5 μg/mL DAPI. Finally, cells were mounted in 90% glycerol in distilled water for microscopic observation. Fluorescence microscope images were acquired using a DeltaVision microscope system (Applied Precision). Three-dimensional optical section images were taken at 0.5-μm focus intervals and computationally processed using SoftWoRx software (Applied Precision).

Acknowledgements

We thank H. Niwa for the original SAiresBlas cassette, M. Nakao for the GFP-MBD plasmid, M. Oda for suggestions regarding ES cell characterization, and D. Sipp, M. Royle and S. Hayashi for critical reading. This work was supported in part by Grants-in-Aid from the Ministry of Education, Culture, Sports, Science, and Technology of Japan.

References

Bachman, K.E., Park, B.H., Rhee, I., *et al.* (2003) Histone modifications and silencing prior to DNA methylation of a tumor suppressor gene. *Cancer Cell* **3**, 89–95.

Bird, A. (2002) DNA methylation patterns and epigenetic memory. *Genes Dev.* **16**, 6–21.

Bourc'his, D. & Bestor, T.H. (2004) Meiotic catastrophe and retrotransposon reactivation in male germ cells lacking Dnmt3L. *Nature* **431**, 96–99.

Chen, T., Ueda, Y., Dodge, J.E., Wang, Z. & Li, E. (2003) Establishment and maintenance of genomic methylation patterns in mouse embryonic stem cells by Dnmt3a and Dnmt3b. *Mol. Cell. Biol.* **23**, 5594–5605.

Clark, S.J., Harrison, J., Paul, C.L. & Frommer, M. (1994) High sensitivity mapping of methylated cytosines. *Nucleic Acids Res.* **22**, 2990–2997.

Dodge, J.E., Okano, M., Dick, F., *et al.* (2005) Inactivation of *Dnmt3b* in mouse embryonic fibroblasts results in DNA hypomethylation, chromosomal instability, and spontaneous immortalization. *J. Biol. Chem.* **280**, 17986–17991.

Eden, A., Gaudet, F., Waghmare, A. & Jaenisch, R. (2003) Chromosomal instability and tumors promoted by DNA hypomethylation. *Science* **300**, 455.

Feinberg, A.P., Ohlsson, R. & Henikoff, S. (2006) The epigenetic progenitor origin of human cancer. *Nat. Rev. Genet.* **7**, 21–33.

Fujita, N., Takebayashi, S., Okumura, K., *et al.* (1999) Methylation-mediated transcriptional silencing in euchromatin by methyl-CpG binding protein MBD1 isoforms. *Mol. Cell. Biol.* **19**, 6415–6426.

Fujita, N., Watanabe, S., Ichimura, T., *et al.* (2003) Methyl-CpG binding domain 1 (MBD1) interacts with the Suv39h1-HP1 heterochromatic complex for DNA methylation-based transcriptional repression. *J. Biol. Chem.* **278**, 24132–24138.

Gaudet, F., Hodgson, J.G., Eden, A., *et al.* (2003) Induction of tumors in mice by genomic hypomethylation. *Science* **300**, 489–492.

Hajkova, P., Erhardt, S., Lane, N., *et al.* (2002) Epigenetic reprogramming in mouse primordial germ cells. *Mech. Dev.* **117**, 15–23.

Hata, K., Kusumi, M., Yokomine, T., Li, E. & Sasaki, H. (2006) Meiotic and epigenetic aberrations in *Dnmt3L*-deficient male germ cells. *Mol. Reprod. Dev.* **73**, 116–122.

Hong, Y. & Stambrook, P.J. (2004) Restoration of an absent G_1 arrest and protection from apoptosis in embryonic stem cells after ionizing radiation. *Proc. Natl. Acad. Sci. USA* **101**, 14443–14448.

Jackson, M., Krassowska, A., Gilbert, N., *et al.* (2004) Severe global DNA hypomethylation blocks differentiation and induces histone hyperacetylation in embryonic stem cells. *Mol. Cell. Biol.* **24**, 8862–8871.

Jackson, J.P., Lindroth, A.M., Cao, X. & Jacobsen, S.E. (2002) Control of CpNpG DNA methylation by the KRYPTONITE histone H3 methyltransferase. *Nature* **416**, 556–560.

Jackson-Grusby, L., Beard, C., Possemato, R., *et al.* (2001) Loss of genomic methylation causes p53-dependent apoptosis and epigenetic deregulation. *Nat. Genet.* **27**, 31–39.

Jenuwein, T. & Allis, C.D. (2001) Translating the histone code. *Science* **293**, 1074–1080.

Jones, P.A. & Baylin, S.B. (2002) The fundamental role of epigenetic events in cancer. *Nat. Rev. Genet.* **3**, 415–428.

Jones, P.L., Veenstra, G.C.J., Wade, P.A., *et al.* (1998) Methylated DNA and MeCP2 recruit histone deacetylase to repress transcription. *Nat. Genet.* **19**, 187–191.

Kimura, H., Tada, M., Nakatsuji, N. & Tada, T. (2004) Histone code modifications on pluripotential nuclei of reprogrammed somatic cells. *Mol. Cell. Biol.* **24**, 5710–5720.

Lehnertz, B., Ueda, Y., Derijck, A.A.H.A., *et al.* (2003) *Suv39h*-mediated histone H3 lysine 9 methylation directs DNA methylation to major satellite repeats at pericentric heterochromatin. *Curr. Biol.* **13**, 1192–1200.

Lei, H., Oh, S.P., Okano, M., *et al.* (1996) De novo DNA cytosine methyltransferase activities in mouse embryonic stem cells. *Development* **122**, 3195–3205.

Li, E. (2002) Chromatin modification and epigenetic reprogramming in mammalian development. *Nat. Rev. Genet.* **3**, 662–673.

Li, E., Bestor, T.H. & Jaenisch, R. (1992) Targeted mutation of the DNA methyltransferase gene results in embryonic lethality. *Cell* **69**, 915–926.

Ma, Y., Jacobs, S.B., Jackson-Grusby, L., *et al.* (2005) DNA CpG hypomethylation induces heterochromatin reorganization involving the histone variant macroH2A. *J. Cell Sci.* **118**, 1607–1616.

Maison, C. & Almouzni, G. (2004) HP1 and the dynamics of heterochromatin maintenance. *Nat. Rev. Mol. Cell Biol.* **5**, 296–304.

Meshorer, E., Yellajoshula, D., George, E., Scambler, P.J., Brown, D.T. & Misteli, T. (2006) Hyperdynamic plasticity of chromatin proteins in pluripotent embryonic stem cells. *Dev. Cell* **10**, 105–116.

Nan, X., Ng, H.H., Johnson, C.A., *et al.* (1998) Transcriptional repression by the methyl-CpG-binding protein MeCP2 involves a histone deacetylase complex. *Nature* **393**, 386–389.

Ng, H.H., Zhang, Y., Hendrich, B., *et al.* (1999) MBD2 is a transcriptional repressor belonging to the MeCP1 histone deacetylase complex. *Nat. Genet.* **23**, 58–61.

Okano, M., Bell, D.W., Haber, D.A. & Li, E. (1999) DNA methyltransferases Dnmt3a and Dnmt3b are essential for de novo methylation and mammalian development. *Cell* **99**, 247–257.

Ramsahoye, B.H., Biniszkiewicz, D., Lyko, F., Clark, V., Bird, A.P. & Jaenisch, R. (2000) Non-CpG methylation is prevalent in embryonic stem cells and may be mediated by DNA methyltransferase 3a. *Proc. Natl. Acad. Sci. USA* **97**, 5237–5242.

Rhee, I., Bachman, K.E., Park, B.H., *et al.* (2002) DNMT1 and DNMT3b cooperate to silence genes in human cancer cells. *Nature* **416**, 552–556.

Robertson, K.D. (2005) DNA methylation and human diseases. *Nat. Rev. Genet.* **6**, 597–610.

Sarraf, S.A. & Stancheva, I. (2004) Methyl-CpG binding protein MBD1 couples histone H3 methylation at lysine 9 by SETDB1 to DNA replication and chromatin assembly. *Mol. Cell* **15**, 595–605.

Tamaru, H. & Selker, E.U. (2001) A histone H3 methyltransferase controls DNA methylation in *Neurospora crassa*. *Nature* **414**, 277–283.

Tariq, M., Saze, H., Probst, A.V., Lichota, J., Habu, Y. & Paszkowski, J. (2003) Erasure of CpG methylation in *Arabidopsis* alters patterns of histone H3 methylation in heterochromatin. *Proc. Natl. Acad. Sci. USA* **100**, 8823–8827.

Vire, E., Brenner, C., Deplus, R., *et al.* (2006) The Polycomb group protein EZH2 directly controls DNA methylation. *Nature* **439**, 871–874.

Wade, P.A., Gegonne, A., Jones, P.L., Ballestar, E., Aubry, F. & Wolffe, A.P. (1999) Mi-2 complex couples DNA methylation to chromatin remodelling and histone deacetylation. *Nat. Genet.* **23**, 62–66.

Walsh, C.P., Chaillet, J.R. & Bestor, T.H. (1998) Transcription of IAP endogenous retroviruses is constrained by cytosine methylation. *Nat. Genet.* **20**, 116–117.

Xu, G.L., Bestor, T.H., Bourc'his, D., *et al.* (1999) Chromosome instability and immunodeficiency syndrome caused by mutations in a DNA methyltransferase gene. *Nature* **402**, 187–191.

Yan, Q., Huang, J., Fan, T., Zhu, H. & Muegge, K. (2003) Lsh, a modulator of CpG methylation, is crucial for normal histone methylation. *EMBO J.* **22**, 5154–5162.

Zhang, Y., Ng, H.H., Erdjument-Bromage, H., Tempst, P., Bird, A. & Reinberg, D. (1999) Analysis of the NuRD subunits reveals a histone deacetylase core complex and a connection with DNA methylation. *Genes Dev.* **13**, 1924–1935.

Received: 10 February 2006
Accepted: 12 April 2006

Supplementary material

The following supplementary material is available for this article online:

Figure S1 Growth curve analysis for TKO cells.

Figure S2 Chromosome analysis by Giemsa staining for TKO cells.

Table S1 Oligonucleotides used in this study.

JOURNAL OF VIROLOGY, May 2006, p. 4510–4520 Vol. 80, No. 9
0022-538X/06/$08.00+0 doi:10.1128/JVI.80.9.4510–4520.2006

Diverse Effects of Cyclosporine on Hepatitis C Virus Strain Replication

Naoto Ishii,[1]† Koichi Watashi,[1]† Takayuki Hishiki,[1] Kaku Goto,[1] Daisuke Inoue,[1] Makoto Hijikata,[1] Takaji Wakita,[2] Nobuyuki Kato,[3] and Kunitada Shimotohno[1]*

Laboratory of Human Tumor Viruses, Department of Viral Oncology, Institute for Virus Research, Kyoto University, Kyoto,[1] Department of Microbiology, Tokyo Metropolitan Institute for Neuroscience, Tokyo,[2] and Department of Molecular Biology, Okayama University Graduate School of Medicine, Dentistry and Pharmaceutical Sciences, Okayama,[3] Japan

Received 18 December 2005/Accepted 10 February 2006

Recently, a production system for infectious particles of hepatitis C virus (HCV) utilizing the genotype 2a JFH1 strain has been developed. This strain has a high capacity for replication in the cells. Cyclosporine (CsA) has a suppressive effect on HCV replication. In this report, we characterize the anti-HCV effect of CsA. We observe that the presence of viral structural proteins does not influence the anti-HCV activity of CsA. Among HCV strains, the replication of genotype 1b replicons was strongly suppressed by treatment with CsA. In contrast, JFH1 replication was less sensitive to CsA and its analog, NIM811. Replication of JFH1 did not require the cellular replication cofactor, cyclophilin B (CyPB). CyPB stimulated the RNA binding activity of NS5B in the genotype 1b replicon but not the genotype 2a JFH1 strain. These findings provide an insight into the mechanisms of diversity governing virus-cell interactions and in the sensitivity of these strains to antiviral agents.

Hepatitis C virus (HCV), a member of the *Flaviviridae* family, has a positive-strand RNA genome (1, 26). The genome encodes a large precursor polyprotein, which is cleaved by host and viral proteases to generate at least 10 functional viral proteins: core, envelope 1 (E1), E2, p7, nonstructural protein 2 (NS2), NS3, NS4A, NS4B, NS5A, and NS5B (6, 8). NS5B is an RNA-dependent RNA polymerase that is crucial for viral genome replication (1, 26). There is genetic heterogeneity within the HCV genome. Currently, these differences are classified into six genotypes that are further segregated into a series of subtypes (4, 23). In Japan, genotype 1b is predominant; roughly 65% of cases of HCV-related chronic hepatitis involve genotype 1b. By comparison, genotype 2a is present in 17% of these patients (13, 23).

Sustained infection of HCV is the major cause of chronic liver diseases such as chronic hepatitis, liver cirrhosis, and hepatocellular carcinoma (16). Rarely, HCV causes fulminant hepatitis (13). The predominant treatment for HCV-infected patients is interferon (IFN) or polyethylene glycol-conjugated IFN alone or in combination with ribavirin (19, 20). However, alternative anti-HCV therapies are needed because virus is not eliminated in about half of the treated patients (19, 20). Lohmann et al. have developed the HCV subgenomic replicon system, in which an HCV subgenomic replicon autonomously replicates in Huh-7 cells (HCV replicon cells) (18). This replicon comprises the HCV 5′ untranslated region (5′UTR) containing an internal ribosomal entry site (IRES), the neomycin phosphotransferase gene, the encephalomyocarditis virus (EMCV) IRES, the coding region for HCV NS3 through NS5B, and the HCV 3′UTR (subgenomic replicon), but it lacks the coding region for the core and envelope proteins, as well as p7 and NS2 (Fig. 1). Subsequently, a genome-length (full-genome) replicon has been developed. This construct contains a full-genome length of HCV, including the coding regions for the core protein through NS2 (Fig. 1) (5, 10). We can evaluate HCV replication using these subgenomic or genome-length replicon systems. Previously, we established HCV subgenomic replicon cells carrying HCV genotype 1b NN strain (15, 29). We demonstrated that an immunosuppressant, cyclosporine (CsA), has anti-HCV activity in these cells (29). In addition, we determined the molecular mechanism of the anti-HCV effect of CsA on this replicon; cyclophilin B (CyPB), one of the cellular targets of CsA, is a cellular replication cofactor of the HCV genome (31). CyPB interacts with NS5B to promote its RNA binding activity (for a detailed description, see reference 31). CsA is suggested to suppress HCV genome replication by inhibiting the functional association of CyPB with NS5B. Another group also reported anti-HCV function of CsA using a subgenomic replicon of other genotype 1b strain, HCV-N (22). In this study, we demonstrate that CsA also has a strong anti-HCV activity in other available genotype 1b replicons carrying the Con1 and O strains (12, 18).

Recently, Wakita and colleagues reported that a replicon of HCV genotype 2a JFH-1 strain, which was isolated from a case of type-C fulminant hepatitis, has a much stronger level of replication activity than genotype 1b replicons in Huh-7 cells (13, 27). A production system of infectious viral particles was recently established with this high-replication-competent strain (17, 27, 34). This viral strain may acquire a growth advantage compared with many other strains, although the underlying mechanism is unknown. In this study, we described a characteristic difference in the replication of JFH1 compared to that of genotype 1b replicons.

Here, we report that JFH1 replication is less sensitive to CsA than genotype 1b strains, although the interaction of

* Corresponding author. Mailing address: Laboratory of Human Tumor Viruses, Department of Viral Oncology, Institute for Virus Research, Kyoto University, 53 Kawaharacho, Shogoin, Sakyo-ku, Kyoto 606-8507, Japan. Phone: 81-75-751-4000. Fax: 81-75-751-3998. E-mail: kshimoto@virus.kyoto-u.ac.jp.

† N.I. and K.W. contributed equally to this work.

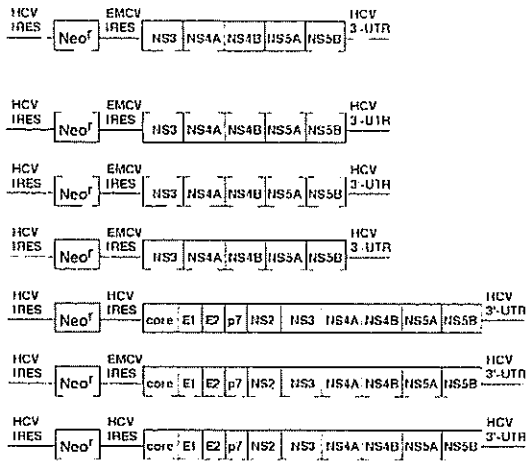

FIG. 1. Schematic representation of the constructs of HCV subgenomic and genome-length replicon RNA. On the left, the constructs of each replicon RNA are shown. HCV strains, as well as genotypes from which the replicon RNA sequences are derived, are indicated in the second column. The names of replicon cell clones established with each replicon RNA are in the third column. The sensitivity to CsA of each replicon RNA revealed in this study is summarized in the fourth column. The replicon RNAs comprise the HCV 5'UTR, including HCV IRES, the neomycin phosphotransferase gene (Neo^r), EMCV IRES, or HCV IRES, the coding region for HCV proteins NS3 to NS5B (subgenomic) or core to NS5B (genome length or full genome), and HCV 3'UTR. MH-14 (NN/1b/SG), #50-1 (NN/1b/SG), MH14#W31 (NN/1b/SG), SN1 (Con1/1b/SG), sO (O/1b/SG), JFH1#4-1 (JFH1/2a/SG), and JFH1#2-3 (JFH1/2a/SG) cells carry subgenomic replicons, while NNC#2 (NN/1b/FL), SN1A#2 (Con1/1b/FL), and SNC#7 (Con1/1b/FL) cells have genome-length replicons. NNC#2 (NN/1b/FL) and SNC#7 (Con1/1b/FL) cells contain the replicon RNA without EMCV IRES.

CyPB with NS5B is observed with this replicon. However, genome replication and RNA binding activity of NS5B are independent of CyPB. We have exploited a chemical compound to demonstrate how strain diversity can be generated by underlying differences in the mechanisms of the virus-cell interaction. These findings provide important insight into the mechanisms that mediate the efficacy of antiviral agents.

MATERIALS AND METHODS

Cell culture. Huh-7 cells were cultured in Dulbecco's modified Eagle medium (Invitrogen) with 10% fetal bovine serum, nonessential amino acids (Invitrogen), and L-glutamine (Invitrogen). MH-14, #50-1, MH14#W31, SN1, sO (formerly named 1B2R1), JFH1#4-1, and JFH1#2-3 cells (12, 13, 15, 18, 29), carrying subgenomic replicons, and NNC#2, SN1A#2, and SNC#7 cells, carrying full-genome replicons, were cultured in the above medium supplemented with 300- to 500-μg/ml G418 (Invitrogen). In the assay measuring the response to CsA, NIM811, or PSC833 (Fig. 2, 3, and 4), we seeded small numbers of each replicon cells (7×10^3 to 15×10^3 cells/12-well plate) and treated with each drug. Culture medium was changed every 3 days (CsA, NIM811, or PSC833 was supplemented in the fresh medium for the treatment groups). We did not perform any passages in the assay period. At day 7, the cells were 70 to 90% confluent. A schematic representation of the constructs of HCV replicon RNAs, the name of HCV strains from which the replicon RNA sequences are derived, and the name of replicon cell clones used in this study are summarized in Fig. 1. Since many replicon clones were used in this study, we list "strain/genotype/length of the replicon construct" in parentheses after the names of each cell clone in Results and in the figure legends to avoid confusion between names: for example, MH-14 (NN/1b/SG), JFH1#4-1 (JFH1/2a/SG), and SN1A#2 (Con1/1b/FL) cells. The designations SG and FL indicate subgenomic and full-genome replicons, respectively.

Establishment of replicon cells. MH-14, #50-1, sO, JFH1#4-1, and JFH1#2-3 cells were described previously (12, 13, 15, 29). The replicon RNAs were produced using a MEGAscript T7 kit (Ambion) from pMH14, pSN1, pNNC, pSN1A, and pSNC plasmids for the establishment of the MH14#W31, SN1, NNC#2, SN1A#2, and SNC#7 replicon cells, respectively. For the establishment of MH14#W31, we transfected RNA into the Huh-7 cell strain which was identical to the parental cells of JFH1#4-1 and JFH1#2-3. Each replicon RNA was transfected into Huh-7 cells, following the selection with the medium in the presence of 500- to 1,000-μg/ml G418 for around 4 weeks. The resultant cell colonies were isolated and expanded. The HCV RNA titers in cell clones carrying JFH1 replicons were not significantly different from those in established cell clones carrying genotype 1b replicons.

Plasmid construction. pSN1, the sequence of which is derived from I377NS3-3' (18), was prepared essentially as described previously (15). pSN1A was generated by inserting the region from the core to NS2 of pM1LE (15) into the upstream coding region for NS3 in pSN1. To obtain pSNC, the EMCV IRES of pSN1A was replaced by the HCV IRES. pNNC was produced by inserting the coding region from NS3 to NS5B of pM1LE into pSNC.

Real-time reverse transcription-PCR (RT-PCR) analysis. The 5'UTR of HCV genome RNA was quantified using the ABI PRISM 7700 sequence detector (Applied Biosystems) as described previously (29).

Immunoblot analysis. Immunoblot analysis was performed as described previously (30). The primary antibodies used in this study were anti-core, anti-E2 (kindly provided by M. Kohara, Tokyo Metropolitan Institute of Medical Science), anti-NS3, anti-NS5A (a generous gift from A. Takamizawa, Osaka University), anti-NS5B (NS5B-6; kindly provided by I. Fukuya, Osaka University), anti-CyPA (Upstate Cell Signaling), anti-CyPB (Affinity BioReagents), and anti-tubulin (Oncogene).

Immunoprecipitation assay and RNA-protein binding precipitation assay. Immunoprecipitation and RNA-protein binding precipitation were performed as described previously (30, 31).

RNA interference technique. The condition of small interfering RNA (siRNA) used in this study was described previously (31). Transfection was performed using siLentFect (Bio-Rad), according to the manufacturer's protocol.

Isolation of replication complex. The HCV replication complex was isolated from cells by treatment with 50-μg/ml digitonin at 27°C for 5 min, following treatment with 0.3-μg/ml proteinase K at 37°C for 5 min as described previously (31).

Purification of recombinant GST-fused CyPB protein. Glutathione *S*-transferase (GST) and GST-fused CyPB (GST-CyPB) protein expression was induced

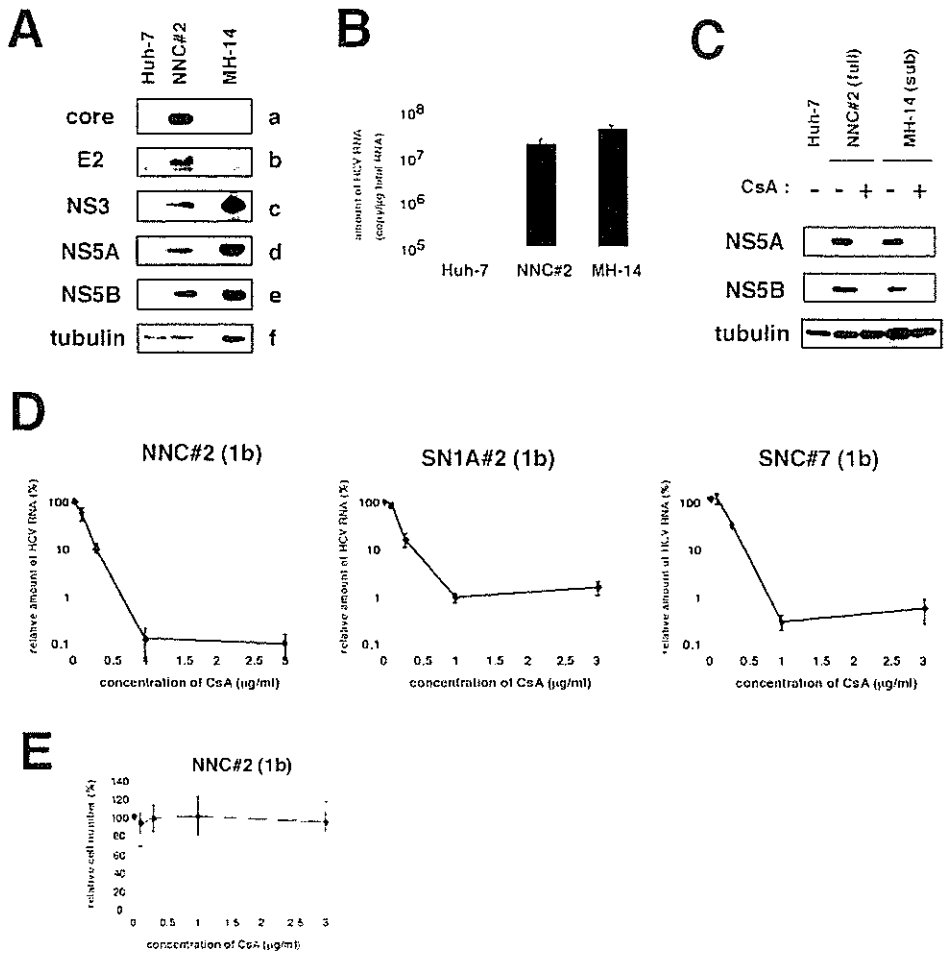

FIG. 2. CsA suppressed the replication of HCV genome, irrespective of the presence of the structural proteins. (A) Detection of HCV proteins from NNC#2 (NN/1b/FL) genome-length replicon. Core (a), E2 (b), NS3 (c), NS5A (d), NS5B (e), and tubulin (f) in Huh-7, NNC#2 (NN/1b/FL), and MH-14 (NN/1b/SG) cells analyzed by immunoblot analysis are shown. (B) HCV RNA in Huh-7, NNC#2 (NN/1b/FL), and MH-14 (NN/1b/SG) cells quantified by real-time RT-PCR analysis. The data represent the means of three independent experiments. (C) CsA decreased the production of HCV proteins in NNC#2 (NN/1b/FL), as well as in MH-14 (NN/1b/SG) cells. After treatment with 1-μg/ml CsA (+) for 5 days or without treatment (−), total-cell lysates of NNC#2 (NN/1b/FL) and MH-14 (NN/1b/SG) cells, together with Huh-7 cells as a negative control, were recovered to examine the production of HCV NS5A (top), NS5B (middle), and tubulin as an internal control (bottom) by immunoblot analysis. The same result was obtained at day 7 after treatment. (D) The sensitivity to CsA of HCV genome-length replicon was almost the same as that of the subgenomic replicon. HCV RNA was quantified by real-time RT-PCR analysis using total RNA from NNC#2 (NN/1b/FL), SN1A#2 (Con1/1b/FL), and SNC#7 (Con1/1b/FL) cells treated with various concentrations of CsA for 7 days. The relative amount of HCV RNA was plotted against the concentration of CsA (in micrograms per milliliter). (E) Effect of CsA on cell proliferation. NNC#2 (NN/1b/FL) cells were treated with various amount of CsA for 7 days. Cell numbers were counted, and cell numbers relative to those of cells without treatment were plotted against the concentration of CsA.

in transformed BL21 cells (Amersham) with 1 mM isopropyl-β-thiogalactopyranoside (IPTG). The cell lysate was incubated with glutathione-Sepharose resin (Amersham) and washed extensively. The recombinant protein was eluted by glutathione (pH 8.0) and subsequently dialyzed.

In vitro RNA binding assay. In vitro-translated ^{35}S-labeled NS5B proteins and poly(U)-Sepharose (Amersham) or protein G-Sepharose (Amersham) resin as a negative control were incubated in the presence of recombinant GST-CyPB protein at 4°C for 1 h. After being washed, precipitates were fractionated by sodium dodecyl sulfate-polyacrylamide gel electrophoresis and analyzed by imaging analyzer.

RESULTS

CsA suppressed the replication of HCV full-genome replicon. We and another group have reported an anti-HCV activity of CsA using subgenomic replicons (22, 29). HCV structural proteins, especially the core protein, have multiple functions. These proteins interact with many cellular factors and modulate a variety of cellular functions (32). Potentially, these viral proteins could diminish or circumvent the suppression of HCV genome replication by CsA. Core protein and E2 reportedly modulate the activity of IFN signaling (9, 25). To test this possibility, we established a full-genome HCV replicon system with cells transfected with the NN strain (NNC#2 cells [NN/1b/FL]) (Fig. 1). HCV RNA and protein productions were confirmed by real-time RT-PCR and immunoblot analysis (Fig. 2A and B). In addition, we confirmed that this replication was not due to the integration of the replicon construct into the

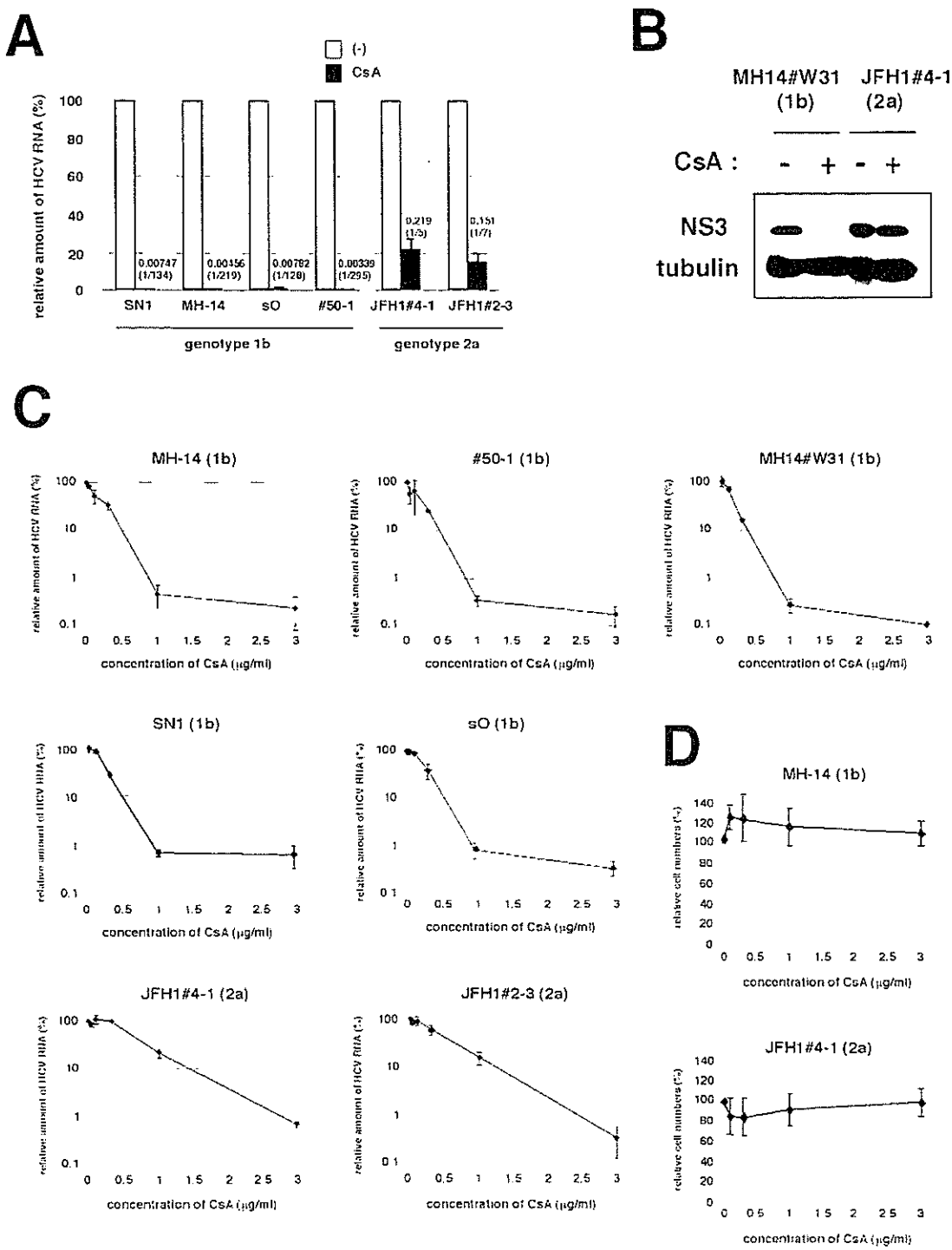

FIG. 3. Replication of a genotype 2a strain, JFH1, was less sensitive to CsA. (A) Sensitivity to CsA of HCV genotype 1b and JFH1 replicons. SN1 (Con1/1b/SG), MH-14 (NN/1b/SG), sO (O/1b/SG), #50-1 (NN/1b/SG), JFH1#4-1 (JFH1/2a/SG), and JFH1#2-3 (JFH1/2a/SG) cells, carrying HCV subgenomic replicon, were treated with 1-μg/ml CsA for 7 days. HCV RNA titers were quantified by real-time RT-PCR analysis, and the relative amounts are shown. The bars represent the means of three independent experiments. White bars, no treatment; black bars, 1-μg/ml CsA. The numbers above the black bars indicate fold difference of the titer with 1-μg/ml CsA treatment compared to no treatment. (B) Levels of NS3 and tubulin as an internal control in MH14#W31 (NN/1b/SG) and JFH1#4-1 (JFH1/2a/SG) cells without (−) or with (+) 1-μg/ml CsA treatment for 5 days were detected by immunoblot analysis. (C) HCV RNA was quantified and plotted as described in the legend to Fig. 2D with genotype 1b replicon cells such as MH-14 (NN/1b/SG), #50-1 (NN/1b/SG), MH14#W31 (NN/1b/SG), SN1 (Con1/1b/SG), and sO (O/1b/SG) cells and JFH1-carrying replicon cells such as JFH1#4-1 (JFH1/2a/SG) and JFH1#2-3 (JFH1/2a/SG) cells. (D) Effect of CsA on cell proliferation. The growth of MH-14 (NN/1b/SG) and JFH1#4-1 (JFH1/2a/SG) cells were examined as described in the legend for Fig. 2E.

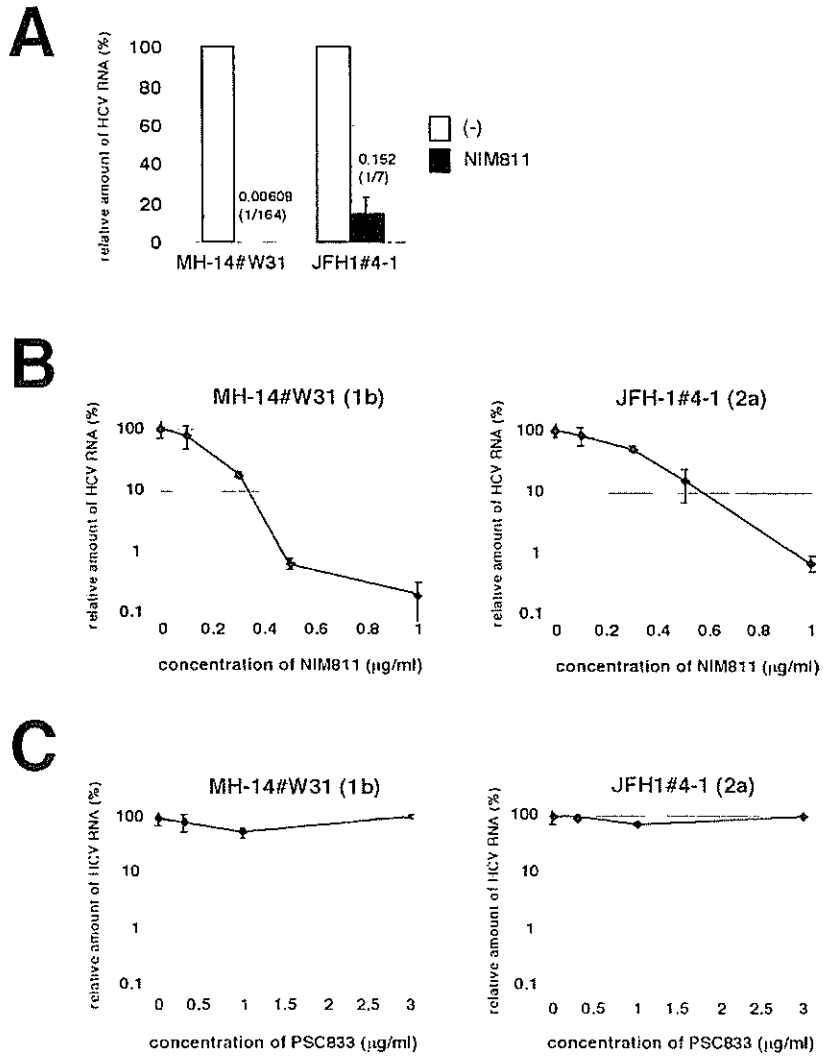

FIG. 4. JFH1 replication was less sensitive to a CsA derivative, NIM811. (A) MH14#W31 (NN/1b/SG) and JFH1#4-1 (JFH1/2a/SG) cells were treated with 0.5-μg/ml NIM811 for 7 days. HCV RNA titers were quantified as described in the legend to Fig. 3A. White bars, no treatment; black bars, 0.5-μg/ml NIM811. (B and C) HCV RNA in replicon cells treated with various concentrations of NIM811 (B) or PSC833 (C) for 7 days was quantified and plotted against the concentration of NIM811 (B) or PSC833 (C) (in micrograms per milliliter) as described in the legend to Fig. 3C.

cellular genome (data not shown). Similarly, we generated other full-genome replicon cells carrying sequences from the Con1 strain at the nonstructural coding region of the replicon RNA (SN1A#2 [Con1/1b/FL]) and SNC#7 (Con1/1b/FL) cells (Fig. 1). The replicon of SN1A#2 (Con1/1b/FL) cells possessed the EMCV IRES upstream of the open reading frame for HCV proteins, while that of SNC#7 (Con1/1b/FL) cells contained the HCV IRES (Fig. 1). SNC#7 (Con1/1b/FL) cells exhibited almost the same response as that of SN1A#2 (Con1/1b/FL) cells to CsA treatment (Fig. 2D). Consistent with a previous report (22), the EMCV IRES was not responsible for the anti-HCV activity of CsA. We compared the sensitivity to CsA of full-genome replicons with that of subgenomic replicons. CsA strongly decreased the production of HCV proteins in both the full-genome replicon, NNC#2 (NN/1b/FL) cells and the subgenomic replicon, MH-14 (NN/1b/SG) cells (Fig. 2C). Real-time RT-PCR analysis also revealed a dramatic reduction of the RNA level of full-genome replicons in NNC#2 (NN/1b/FL), SN1A#2 (Con1/1b/FL), and SNC#7 (Con1/1b/FL) cells (Fig. 2D). The 50% inhibitory concentrations (IC_{50}) of CsA in NNC#2 (NN/1b/FL), SN1A#2 (Con1/1b/FL), and SNC#7 (Con1/1b/FL) cells awere estimated to be 0.13, 0.19, and 0.24 μg/ml, respectively. The 90% inhibitory concentrations (IC_{90}) of CsA in these cells were 0.68, 0.94, and 0.81 μg/ml, respectively. The CsA dose-response curves of full-genome replicons and subgenomic replicons were similar (i.e., compare SN1A#2 or SNC#7 [Con1/1b/FL] versus SN1 [Con1/1b/SG], NNC#2 [NN/1b/FL] versus MH-14, #50-1, or MH14#W31 [NN/1b/SG]) (Fig. 3C). These results demonstrate that CsA suppresses the replication of full-genome replicons and subgenomic replicons to almost the same extent. Since CsA concentrations of up to 3 μg/ml did not affect the

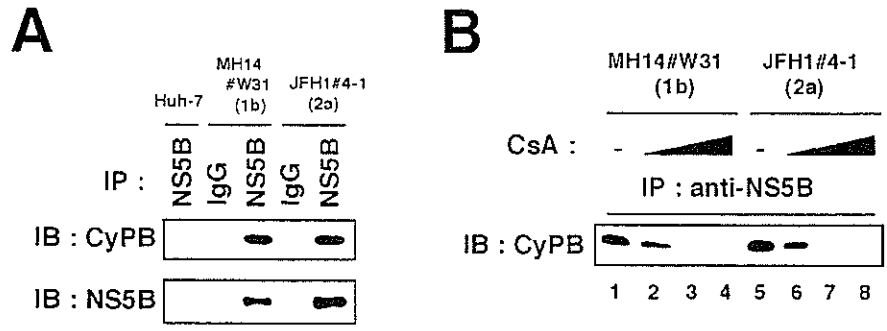

FIG. 5. Interaction of HCV NS5B with CyPB in the JFH1 replicon. (A) Coimmunoprecipitation of endogenous CyPB with NS5B. Lysates from MH14#W31 (NN/1b/SG), JFH1#4-1 (JFH1/2a/SG), and Huh-7 cells as a negative control were used for immunoprecipitation with normal mouse immunoglobulin G (IgG) or anti-NS5B antibody (NS5B), followed by immunoblot analysis with either anti-CyPB (top) or anti-NS5B antibodies (bottom). IP, antibodies used for immunoprecipitation. (B) The interaction of CyPB with NS5B in JFH1 replicon was disrupted by CsA treatment. Coimmunoprecipitation between CyPB and NS5B was analyzed with MH14#W31 (NN/1b/SG) or JFH1#4-1 (JFH1/2a/SG) cells treated without CsA (lanes 1 and 5) or with CsA (0.3 μg/ml in lanes 2 and 6, 1 μg/ml in lanes 3 and 7, and 3 μg/ml in lanes 4 and 8).

proliferation of any replicon cells (Fig. 2E and data not shown), the effect of CsA on replication is not due to the cytotoxic effect. In addition, we observed the reduction of production of infectious viral particles in the presence of 3-μg/ml CsA (data not shown) using the viral production system with full-genome JFH1 RNA (27).

The JFH1 replicon was less sensitive to CsA than were genotype 1b replicons. We compared the sensitivity of HCV replication to CsA in several subgenomic replicon cells. We used MH-14 (NN/1b/SG) and #50-1 (NN/1b/SG) cells carrying subgenomic replicons with HCV NN strain (15, 29), SN1 (Con1/1b/SG) cells carrying the Con1 subgenomic replicon (18), and sO (O/1b/SG) cells bearing the subgenomic O strain (12) as genotype 1b replicon-containing cells. We also employed JFH1#4-1 (JFH1/2a/SG) and JFH1#2-3 (JFH1/2a/SG) cell clones carrying the JFH1 subgenomic replicon (13). Treatment of CsA (1 μg/ml; 7 days) drastically decreased HCV RNA in all the subgenomic replicon cells carrying the HCV genotype 1b strain. HCV RNA levels in SN1 (Con1/1b/SG), MH-14 (NN/1b/SG), sO (O/1b/SG), and #50-1 (NN/1b/SG) cells decreased to 1/134, 1/219, 1/128, and 1/295, respectively (Fig. 3A). Genotype 1b replicon cells appeared highly sensitive to CsA. In contrast, the effect of CsA on HCV RNA levels in replicon cells containing sequences from the JFH1 strain was limited to 1/5 to 1/7 (Fig. 3A). These results of the response to CsA were reproduced in further additional cell clones.

The cellular characteristics of Huh-7 cell strains differ among laboratories. To exclude the possibility that differences between Huh-7 cell strains influence the sensitivity to CsA, we established genotype 1b replicon cells based on the identical Huh-7 cell strain, which were used as parental cells of JFH1#4-1 (JFH1/2a/SG) and JFH1#2-3 (JFH1/2a/SG) cells. The response of the corresponding replicon cells, MH14#W31 (NN/1b/SG), to CsA was almost the same as that of SN1 (Con1/1b/SG), MH-14 (NN/1b/SG), sO (O/1b/SG), and #50-1 (NN/1b/SG) cells (Fig. 3C). Thus, the difference in sensitivity of JFH1 and genotype 1b strains to CsA can be attributed to the characteristic differences of the HCV strains, not to the parental Huh-7 cell strain. In addition, the reduction of NS3 protein in JFH1#4-1 (JFH1/2a/SG) cells following treatment with CsA was less prominent than that in MH14#W31 (NN/1b/SG) cells (Fig. 3B).

We examined the dose-response curve of HCV RNA against the concentration of CsA (Fig. 3C). The effect of CsA in genotype 1b replicons plateaued at around 1 μg/ml, while in the dose-response curve in JFH1 replicon, the inhibition was not yet saturated (Fig. 3C). As concentrations of CsA up to 3 μg/ml did not affect the proliferation rate of any replicon cells (Fig. 3D and data not shown), the effect of CsA on replication was not due to the cytotoxic effect. The IC_{50} of CsA in MH-14 (NN/1b/SG), #50-1 (NN/1b/SG), MH14#W31 (NN/1b/SG), SN1 (Con1/1b/SG), sO (O/1b/SG), JFH1#4-1 (JFH1/2a/SG), and JFH1#2-3 (JFH1/2a/SG) cells were estimated to be 0.15, 0.18, 0.16, 0.20, 0.25, 0.67, and 0.43 μg/ml, respectively. The IC_{90} was 0.86, 0.82, 0.76, 0.88, 0.92, 2.77, and 2.39 μg/ml, respectively. A similar dose-response curve in the JFH1 replicon was obtained by a transient replication assay with the luciferase reporter driven from a JFH1 replicon construct (data not shown) (14).

JFH1 replicon was less sensitive to a CsA derivative, NIM811. Analysis of several CsA derivatives has revealed that the anti-HCV effect of CsA on the genotype 1b replicon is mediated by the inhibition of CyP (31). We examined the sensitivity of JFH1 replicon to CsA derivatives. CsA is known to have three major cellular targets: CyP, calcineurin (CN)/NF-AT, and P glycoprotein (P-gp) (28, 31). A CsA derivative, NIM811, inhibits CyP and P-gp but not CN/NF-AT, while another derivative, PSC833, inhibits P-gp but neither CyP nor CN/NF-AT (31). The decrease of HCV RNA in MH14#W31 (NN/1b/SG) cells with NIM811 treatment (0.5 μg/ml; 7 days) was more than an order of magnitude greater than that in JFH1#4-1 (JFH1/2a/SG) cells (Fig. 4A). The slope of the dose-response curve of NIM811 treatment of the JFH1 replicon was gentler than that of genotype 1b (Fig. 4B). The IC_{50} of NIM811 in MH14W#31 (NN/1b/SG) and JFH1#4-1 (JFH1/2a/SG) cells were 0.17 and 0.30 μg/ml, respectively. The IC_{90} were 0.46 and 0.93 μg/ml, respectively. In contrast, PSC833, which does not inhibit CyP, did not alter HCV RNA level in either genotype 1b or the JFH1 replicon (Fig. 4C). Thus, a CyP

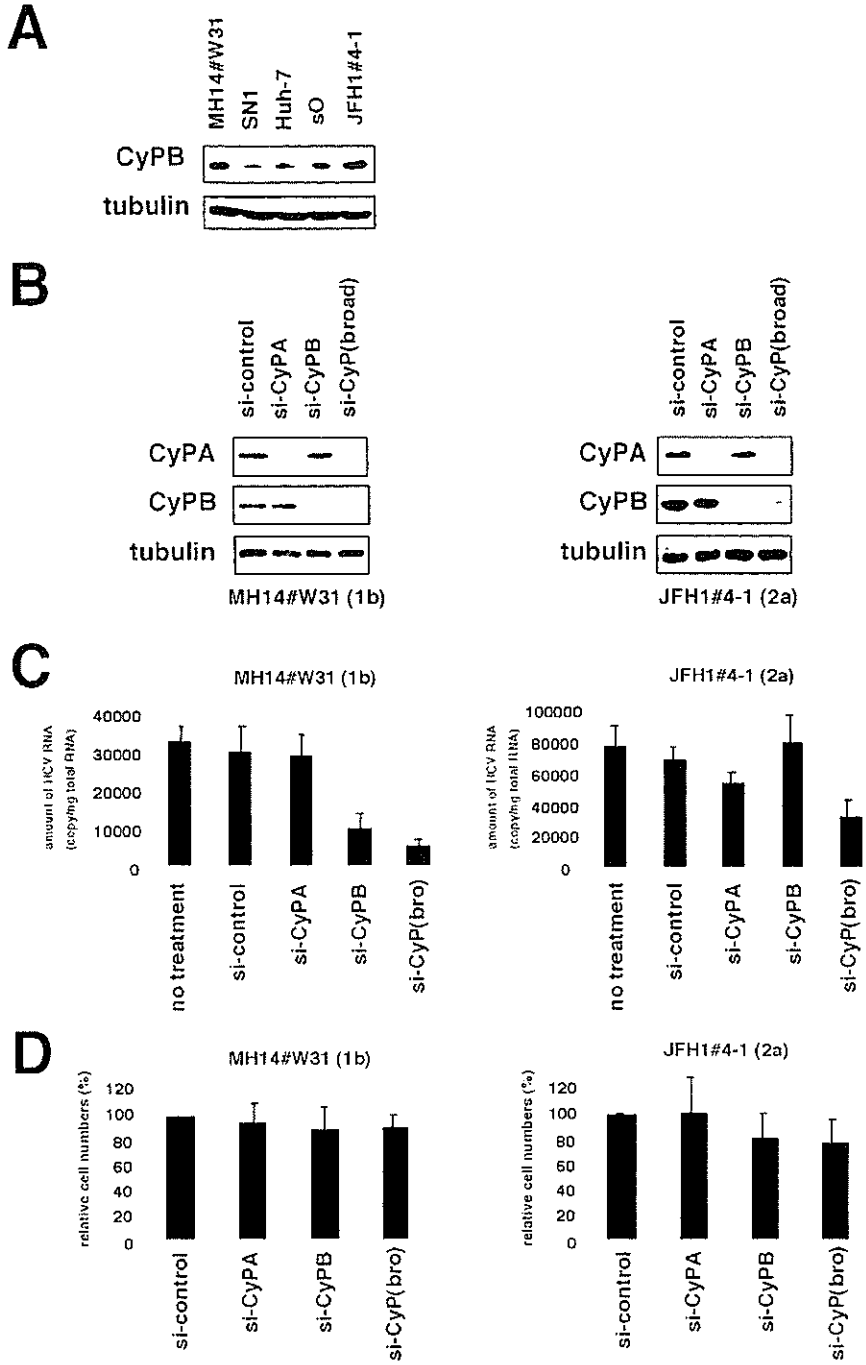

FIG. 6. CyPB in HCV replication of genotype 1b and JFH1. (A) Expression level of endogenous CyPB protein (top) and tubulin as an internal control (bottom) in MH14#W31 (NN/1b/SG), SN1 (Con1/1b/SG), sO (O/1b/SG), JFH1#4-1 (JFH1/2a/SG), and Huh-7 cells. (B) Knockdown of endogenous CyP proteins. MH14#W31 (NN/1b/SG) and JFH1#4-1 (JFH1/2a/SG) cells were transfected with siRNA specific for CyPA (si-CyPA), CyPB (si-CyP), a broad range of CyP subtypes [si-CyP(broad)], or a randomized siRNA (si-control). At 72 h posttransfection, CyPA (top), CyPB (middle) and tubulin as an internal control (bottom) were detected in total cell lysates of MH14#W31 (NN/1b/SG) (left) and JFH1#4-1 (JFH1/2a/SG) (right) cells by immunoblot analysis. (C) Depletion of CyPB did not affect HCV replication of JFH1 replicon. At 5 days posttransfection, HCV RNA titers in MH14#W31 (NN/1b/SG) (left) and JFH1#4-1 (JFH1/2a/SG) (right) cells were quantified by real-time RT-PCR analysis. no treatment, treatment with only the transfection reagent in the absence of siRNA. (D) Effect of siRNA on cell proliferation. Cell numbers of MH14W#31 (NN/1b/SG) and JFH1#4-1 (JFH1/2a/SG) cells treated with siRNA for 5 days were counted. Relative cell numbers were indicated.